OXFORD

G3 Genes | Genomes | Genetics

G3, 2021, 11(2), jkab013
DOI: 10.1093/g3journal/jkab013
Advance Access Publication Date: 23 January 2021
Investigation

KH domain containing RNA-binding proteins coordinate with microRNAs to regulate *Caenorhabditis elegans* development

Dustin Haskell and Anna Zinovyeva*

Division of Biology, Kansas State University, Manhattan, KS 66506, USA

*Corresponding author: Division of Biology, Kansas State University, 28 Ackert Hall, 1717 Claflin Road, Manhattan, KS 66506, USA. zinovyeva@ksu.edu

Abstract

MicroRNAs (miRNAs) and RNA-binding proteins (RBPs) regulate gene expression at the post-transcriptional level, but the extent to which these key regulators of gene expression coordinate their activities and the precise mechanisms of this coordination are not well understood. RBPs often have recognizable RNA binding domains that correlate with specific protein function. Recently, several RBPs containing K homology (KH) RNA binding domains were shown to work with miRNAs to regulate gene expression, raising the possibility that KH domains may be important for coordinating with miRNA pathways in gene expression regulation. To ascertain whether additional KH domain proteins functionally interact with miRNAs during *Caenorhabditis elegans* development, we knocked down twenty-four genes encoding KH-domain proteins in several miRNA sensitized genetic backgrounds. Here, we report that a majority of the KH domain-containing genes genetically interact with multiple miRNAs and Argonaute *alg-1*. Interestingly, two KH domain genes, predicted splicing factors *sfa-1* and *asd-2*, genetically interacted with all of the miRNA mutants tested, whereas other KH domain genes showed genetic interactions only with specific miRNAs. Our domain architecture and phylogenetic relationship analyses of the *C. elegans* KH domain-containing proteins revealed potential groups that may share both structure and function. Collectively, we show that many *C. elegans* KH domain RBPs functionally interact with miRNAs, suggesting direct or indirect coordination between these two classes of post-transcriptional gene expression regulators.

Keywords: microRNA; RNA-binding protein; KH domain; hnRNPK

Introduction

Most developmental and cellular processes rely on precise choreography of gene regulatory networks that incorporate a wide range of cellular and environmental inputs. Evolution of multiple regulatory pathways provided cells with multifaceted and combinatorial methods of regulating gene expression allowing for robustness, flexibility, and rapid remodeling of expression patterns. One of the essential layers of gene regulation occurs at the post-transcriptional level and is effected by two classes of molecules: small noncoding RNAs called microRNAs (miRNAs) and RNA-binding proteins (RBPs). The human genome is predicted to encode at least 2000 miRNAs (Alles *et al.* 2019) and approximately 1500 RBPs (Gerstberger *et al.* 2014). In comparison, *C. elegans* genome is predicted to encode more than 180 miRNAs (Ambros and Ruvkun 2018) and at least 850 RBPs (Tamburino *et al.* 2013), making it a more tractable model to study the genetic interactions between miRNAs and RBPs.

Most mature miRNAs are generated via a canonical multi-step biogenesis pathway that starts with transcription of primary miRNA (pri-miRNA) transcripts (reviewed in Gebert and MacRae 2019). Pri-miRNAs are then processed by consecutive enzymatic activities of Drosha and Dicer endonucleases to generate a double-stranded RNA duplex, which is ultimately loaded into an Argonaute protein. A single miRNA strand is retained by an Argonaute and the mature miRNA silencing complex (miRISC) is formed when the miRNA-loaded Argonaute associates with a GW182 effector on the target messenger RNA (mRNA) (reviewed in Gebert and MacRae 2019). The miRISC identifies target mRNAs through partial sequence complementarity, ultimately resulting in translation repression and/or mRNA degradation (reviewed in O'Brien *et al.* 2018; Gebert and MacRae 2019).

RNA-binding proteins regulate diverse aspects of mRNA life-cycle, including splicing, transport, and stability (Dassi 2017). Diversity in protein architecture and auxiliary domains, as well as a high degree of modularity, allows RBPs to impart specific and potent effects on the gene expression of their targets (Janga 2012). For example, the PUF family of proteins in *C. elegans* inhibits translation of their mRNA targets through sequence-specific binding of the 3′UTR in order to promote deadenylation or by physically blocking cap recognition by translation initiation factors (reviewed in Wang and Voronina 2020). Other proteins like OMA-1 appear to play a more nuanced role by concomitantly binding the 3′UTRs of mRNAs along with translational repressors like LIN-41 to mediate the selective repression-to-activation

Received: July 30, 2020. **Accepted:** December 23, 2020

transition for a subset of mRNAs essential for oogenesis (Tsukamoto *et al.* 2017). Here, RBPs and miRNAs are thought to cooperate extensively, and de-regulation of their activity can precipitate widespread disruption of gene regulatory networks resulting in a variety of cell pathologies and disease states (Tüfekci *et al.* 2013; O'Brien *et al.* 2018).

To effect post-transcriptional regulation of gene expression, RBP and miRNA activity can intersect on multiple levels. On a most basic level, miRNA biogenesis is performed and aided by RBPs (reviewed in Gebert and MacRae 2019). RBPs may directly associate with miRNA-target complexes to modulate the downstream effects on target gene expression (Hammell *et al.* 2009; Schwamborn *et al.* 2009; Wu *et al.* 2017). Coordination between RBPs and miRNAs can also be indirect, with individual factors affecting the target mRNA in distinct ways, ultimately resulting in a unique combinatorial gene regulatory outcome.

Among RBPs identified as modulators of miRNA activity are three proteins that share a conserved RNA-binding K-homology (KH) domain (Akay *et al.* 2013; Zabinsky *et al.* 2017; Li *et al.* 2019). KH domain was first described in human hnRNP K (Siomi *et al.* 1993, reviewed in Geuens *et al.* 2016) and is present alone or in tandem in a large group of RBPs associated with transcription or translation regulation (Nicastro *et al.* 2015; Dominguez *et al.* 2018). The type I KH domain, found in eukaryotes, is approximately 70 amino acids and is characterized by three anti-parallel beta-sheets abutted by three alpha-helices; it includes the GXXG loop, which is thought to be responsible for nucleic acid binding (Grishin 2001; Valverde *et al.* 2008). We recently showed that HRPK-1, a KH domain-containing protein, physically and functionally interacts with miRNA complexes to modulate gene expression during *C. elegans* development (Li *et al.* 2019). Similarly, the KH domain protein VGLN-1 genetically interacts with a diverse set of miRNAs involved in early embryonic and larval development (Zabinsky *et al.* 2017). VGLN-1 binds mRNAs rich with miRNA binding sites in their 3′UTR (Zabinsky *et al.* 2017) and may serve as a platform, bridging interactions between multiple miRNAs, mRNAs, and proteins to regulate gene expression (Zabinsky *et al.* 2017). GLD-1, an RNA-binding protein and a well-characterized translational repressor that regulates germline development (Marin and Evans 2003), has been shown to genetically interact with multiple miRNAs (Akay *et al.* 2013). GLD-1 contains a single KH domain, functionally interacts with miRNA modulators, *nhl-1* and *vig-1*, and physically interacts with ALG-1, CGH-1, and PAB-1, proteins that are key for miRNA gene regulatory activity (Akay *et al.* 2013). Collectively, these findings suggest that RBPs that harbor KH domain(s) may be functionally important for miRNA-dependent gene regulation.

To determine the extent of functional coordination between the KH domain-containing proteins and miRNAs, we knocked down 24 additional predicted *C. elegans* KH domain genes in sensitized miRNA genetic backgrounds. Strikingly, knockdown of 18 KH domain genes resulted in a modulation of a phenotype associated with a partial loss of miRNA activity. We found that several genes, including the predicted splicing factors *sfa-1* and *asd-2*, genetically interacted with multiple miRNA families, suggesting that splicing events may influence miRNA gene regulatory activity. Other genes, such as *Y69A2AR.32*, showed miRNA family specificity. Knockdown of most KH domain genes resulted in enhancement of miRNA reduction-of-function phenotypes, suggesting a normally positive functional interaction between KH domain RBPs and miRNAs. However, knockdown of several genes resulted in mild to strong suppression of defects observed in an Argonaute *alg-1* antimorphic mutant, suggesting that some of these factors normally act antagonistically to miRNAs. Overall, this work provides a comprehensive examination of the genetic interactions between miRNAs and KH domain RBPs in *C. elegans*, presents a phylogenetic and a domain analysis of *C. elegans* KH domain-containing proteins, and suggests that these RBPs may directly or indirectly coordinate with miRNA pathways to regulate gene expression.

Materials and methods

Worm strains

Worm culture and maintenance was performed as previously described (Brenner 1974). Bristol N2 was used as the wild-type strain. Strains used in this study are OH3646 *lsy-6(ot150)*; *otIs114 [Plim-6-gfp + rol-6(su1006)]*, OH812 *otIs114 [Plim-p-gfp + rol-6(su1006)]*, PS3662 *syIs63 [cog-1::gfp + unc-119(+)]*, OH7310 *otIs193 [Pcog-1::lsy-6 + rol-6(su1006)]; sy1s63*, VT1296 *mir-48 mir-241(nDf51) col-19::gfp (maIs105)*, MT7626 *let-7(n2853)*, VT2223 *lin-31(n1053); col-19::gfp (maIs105)*; *alg-1(ma202)*, HW1113 [*Pdpy-30::GFP(PEST)-H2B::lin-41* 3'UTR (*xeSi78*); *Pdpy-30::mCherry::H2B*::artificial 3'UTR (*xeSi36*)], HW1114 [*Pdpy-30::GFP(PEST)-H2B::lin-41* 3'UTR (*xeSi78*); *Pdpy-30::mCherry::H2B*::artificial 3'UTR (*xeSi36*), *let-7(n2853)*], HW1159 [*Pdpy-30::GFP(PEST)-H2B::lin-41* delta LCS 3'UTR (*xeSi87*); *Pdpy-30::mCherry::H2B*::artificial 3'UTR (*xeSi36*)], and BW1932 *hbl-1p::gfp::NLS::hbl-1* 3'UTR (*ctIS39*). All strains were grown at 20°C with the exception of MT7626 *let-7(n2853)* which was grown and maintained at 15°C to prevent excess bursting.

RNA interference

RNAi constructs (pL4440) were obtained from the Ahringer RNAi library (Kamath *et al.* 2000; Source Biosciences) except for *bcc-1* and *E02D9.1* which were obtained from the Vidal RNAi library (Rual *et al.* 2004; Source Biosciences). In addition, 3 RNAi clones were constructed by genomic amplification of the endogenous loci and cloning of the fragment into the L4440 vector. The *fubl-3* clone was generated by using forward 5′-GCCCACTAGTGGAC TAACTGCAACGTTCAA-3′ and reverse 5′-GTGGGTACCATTTGC CGCCTCAGAATTG-3′. The *Y6A2AR.32* clone was generated using forward 5′-GCTCAGATCTTGCCACGTTTCATGCGAAAC-3′ and reverse 5′-GTAGGTACCGGAAGCTCTTCCTCTCACAA-3′. The *B0280.17* clone was generated using forward 5′-GGCCAGATCTC TTCTAGTTCGTGAAATCAA-3′ and reverse 5′-ATAGGTACCGCA GTCTCGGGAGGAAAG-3′. The amplified genomic fragments containing restriction sites were digested using *SpeI* and *Kpn*1 (*fubl-3*) or *Bgl*II and *Kpn*I (*Y69A2AR.32 and B0280.17*) and were ligated with the digested L4440 vector using NEB (M2200) Quick Ligation protocol. Ligated plasmid was then transformed into *E. coli* HT115 bacteria. Sequence insertion into the L4440 plasmid was confirmed via Sanger sequencing (using M13 forward sequencing primer). Although the Ahringer clone targeting *mex-3* was obtained, RNAi of *mex-3* in *lsy-6(ot150)* and *mir-48 mir-241(nDf51)* resulted in highly penetrant embryonic lethality preventing scoring of the F1 progeny of the RNAi treated animals.

RNAi experiments were done by feeding and performed at 20°C unless otherwise stated and as described below. All RNAi experiments of individual genes were performed in parallel with empty vector RNAi (negative control). *dcr-1* RNAi was used as a positive control as loss or reduction of *dcr-1* eliminates/impairs miRNA biogenesis. RNAi plates were prepared and seeded using standard methods (Kamath *et al.* 2000). Scoring requiring fluorescence was done on a Leica DM6B fluorescent compound microscope. Imaging of fluorescence-based phenotypes was done using the Leica DM6B mounted camera and processed using Leica

software. Photoplates were assembled using Adobe Illustrator. Scoring of vulval bursting, brood size, and embryonic lethality were done a standard Leica dissecting microscope. The number of animals scored per replicate as well as the percentage of animals displaying the abnormal phenotype in each replicate are reported in Supplementary Tables S1 and S2.

Despite the overall relatedness of protein architecture among member of phylogenetic clades (Figure 8), BLAST (NCBI) searches for RNAi-targeted regions suggest there is sufficient variation in nucleotide sequence for individual RNAi clones to specifically target the gene of choice. The rare exceptions may be the *fubl* genes, and the *asd-2/gld-1* pair which show a very low level of overlap in targeted sequence, allowing for the possibility that some cross-gene RNAi targeting may occur.

ASEL cell fate differentiation

Plim-6::gfp (otIs114) and *lsy-6(ot150)*; *Plim-6::gfp (otIs114)* worms were placed on RNAi as embryos and F1 progeny were scored as L4 or young adults to increase the ease of detecting fluorescent signal in ASEL neurons. Each group of genes was scored alongside the negative control (empty L4440 vector) and our positive control (*dcr-1* RNAi). Worms were scored as cell fate defective when *lim-6::gfp* was undetectable in the ASEL neuron soma.

Uterine *cog-1::gfp*

cog-1::gfp (syIs63) and *cog-1::gfp (syIs63); otIs193[Pcog-1::lsy-6; rol-6(su1006)]* worms were placed on RNAi as embryos and F1 progeny were scored at mid-late L4s in order to ensure a strong GFP signal in both vulval and uterine cells. Each group of genes was scored alongside the negative control (empty L4440 vector) and our positive control (*dcr-1* RNAi). Worms were considered to have abnormal uterine *cog-1::gfp* if either the anterior or posterior or both uterine cells were lacking GFP. *cog-1* expression was scored as normal when GFP expression was observed in both uterine cells and in vulval cells.

Hypodermal *col-19::gfp* expression and seam cell number

col-19::gfp (maIs105) and *mir-48 mir-241(nDf51) col-19::gfp (maIs105)* animals were placed on RNAi as young L4s and their F1 progeny were scored as young adults. Each group of genes was scored alongside the negative control (empty L4440 vector) and our positive control (*dcr-1* RNAi). Worms were scored first for the presence of *col-19::gfp* in the hypodermal cells. Normal expression was defined as all hypodermal cells expressing *col-19::gfp*, whereas abnormal expression was defined as GFP signal absent in many or all of hypodermal cells. Worms were also scored for the number of seam cells present between the pharynx and rectal cells; seam cells were identified using the *col-19::gfp* transgene. *lin-31(n1053)*, *col-19::gfp (maIs105)*; *alg-1(ma202)* worms were scored in an identical manner when assaying hypodermal *col-19::gfp* expression.

hbl-1::gfp expression

hbl-1p::gfp::NLS::*hbl-1* 3′UTR (*ctIS39*) animals were synchronized by bleaching and plated on RNAi plates with the RNAi bacteria supplemented with fluorescent beads for accurate staging (Nika *et al.* 2016). Worms were grown until the majority began the L2 molt, at which point worms were screened for the presence of fluorescent beads within the gut. Worms that lacked beads and therefore had entered the L2 molt were picked to a new plate seeded with the equivalent RNAi bacteria without beads. The molting worms were then screened every 30 minutes for resumption of pumping indicating they had exited the molt into L3. The worms were then scored at 40x magnification for *hbl-1::gfp* expression in hypodermal cells. Representative images were taken at 63X magnification.

Vulval bursting

let-7(n2853) worms were grown and maintained at 15°C. Embryos were synchronized by hypochloride/NaOH solution and embryos plated directly onto RNAi plates as previously described (Parry *et al.* 2007). The embryos were hatched and grown at 15°C until young adults. Worms were scored for vulval bursting ~6 h after the L4 molt to ensure all animals had reached adulthood. Each group of genes was scored alongside the negative control (empty L4440 vector) and our positive control (*dcr-1* RNAi).

lin-41 reporter assay

[*Pdpy-30::GFP(PEST)-H2B::lin-41* 3′UTR (*xeSi78*); *Pdpy-30::mCherry::H2B*::artificial 3′UTR (*xeSi36*)] (HW1113), [*Pdpy-30::GFP(PEST)-H2B::lin-41* 3′UTR (*xeSi78*); *Pdpy-30::mCherry::H2B*::artificial 3′UTR (*xeSi36*), *let-7(n2853)*] (HW1114), [*Pdpy-30::GFP(PEST)-H2B::lin-41* delta LCS 3′UTR (*xeSi87*); *Pdpy-30::mCherry::H2B*::artificial 3′UTR (*xeSi36*)] (HW1159) (Ecsedi *et al.* 2015) animals were synchronized by bleaching. Embryos were plated onto seeded RNAi plates. Worms were grown until L4 at which point they were imaged at 63x magnification in red and green channels to capture GFP and mCherry expression in the vulval cells. Leica image analysis software was used to determine the fluorescence in each region of interest (ROI) surrounding each of six vulval cells in both red and green channels. Identical exposure and microscope settings were used for all imaging to allow quantification and comparison of signals. To quantify the changes in *lin-41* expression we divided the relative signal intensity of the green channel by the signal intensity in the red channels in each of the vulval cells. The average signal intensity for the vulval tissue was determined by averaging the signal ratios across the six cells scored for each worm. The representative images were adjusted for brightness and contrast post-quantification to allow the reader to more easily observe the fluorescence in cells of interest.

Brood size and embryonic lethality

Wildtype (N2) worms were placed on RNAi as L4s and allowed to lay embryos. When the F1 progeny reached the L4 stage, individual hermaphrodites were moved to their own RNAi plates and allowed to lay embryos for 24 h. After 24 h, each animal was moved to a fresh RNAi plate each day for three additional days. Live larvae were counted on each plate (by picking) 24 and 48 h after the parent has been moved to ensure all larvae were counted. Dead embryos on each plate were counted 48 h after removal of the parent. The total number of live larvae and dead embryos for each hermaphrodite was tallied and together encompass brood size. Embryonic lethality was calculated as (# dead embryos/total brood size) × 100%. Larval arrest was rarely seen, but when it did occur these worms were counted as "live larvae" because they had successfully hatched and developed beyond the embryonic stage.

Phylogenetic analysis

Full proteins sequences of the longest isoforms for each protein were collected from Wormbase and entered to the Mega X program. A MUSCLE protein alignment was carried out to provide input for further phylogenetic analysis. In order to construct the tree, we selected the Maximum Likelihood method and

bootstrapped the tree-building (1000 iterations) to increase the stringency of the method. A simple LG model was selected for the substitution model, using a Nearest-Neighbor-Interchange (NNI) method. The phylogenic tree shown represents 27 of the 28 KH domain proteins in the *C. elegans* genome: *mask-1* was excluded due to extensive length and sequence/domain variability from the rest of the protein family.

Protein domain and architecture

To generate the protein domain graphics, we first determined the longest isoform of each individual protein. The amino acid sequence of the proteins were obtained from Wormbase.org and entered into Simple Modular Architecture Research Tool (SMART) (Letunic and Bork 2017) under the Genomic options. Domain start and end points were noted and used to generate the proteins graphics in Adobe Illustrator.

To generate the coverage of each RNAi clone used in this study, primer pairs were obtained from the Ahringer library database, aligned to the appropriate transcript. Each RNAi target was then translated in the appropriate frame and aligned to the complete protein sequence. Predicted NLS sites were determined using cNLS Mapper using a threshold of 5.0 (Kosugi *et al.* 2009). Only high confidence (score > 8.0) NLS regions were included in the domain graphics.

Statistical analysis

All statistics were done using GraphPad Prism software. Statistical significance was determined using a one-way ANOVA test. To make the desired comparisons and avoid the loss of statistical power inherent to multiple comparisons, we used planned comparisons to compare each individual gene RNAi with vector control RNAi. Bonferroni correction was applied as a post hoc analysis.

Data availability

Strains and plasmids are available upon request. All data necessary for confirming the finding of this article are present within the article and the associated figures, and tables. Supplementary material is available at figshare: https://doi.org/10.25387/g3.13551626.

Results

Multiple KH domain genes genetically interact with *lsy-6* miRNA in ASEL neuronal cell fate specification

The *lsy-6* miRNA controls cell fate specification of the ASEL/ASER sensory neuron pair. *lsy-6* normally represses expression of *cog-1* in the ASEL neuron, ultimately resulting in an ASEL specific gene expression pattern (Johnston and Hobert 2003) (Figure 1A). Loss of *lsy-6* activity results in an inappropriate cell fate switch of the ASEL neuron to the ASER cell fate (Johnston and Hobert 2003). The *lsy-6(ot150)* reduction-of-function mutation causes a low penetrance phenotype, with ~15% of *lsy-6(ot150)* animals displaying an ASEL cell fate defective phenotype. This cell fate defect can be observed by the loss of the *Plim-6::gfp* expression within the ASEL neuron (Figure 1, A and B).

To identify whether KH-domain genes play a role in *lsy-6*-dependent neuronal cell fate specification, we knocked down twenty-four KH domain genes in the *lsy-6(ot150)* mutant background (Figure 1B) and assayed the penetrance of the ASEL cell fate defect. Knockdown of five of the KH domain genes, *pes-4, sfa-1, mask-1, F54D1.1*, and *asd-2* significantly enhanced the *lsy-6(ot150)* cell fate defective phenotype (Figure 1B and Table 1). RNAi-mediated knockdown of the KH domain genes did not result in a phenotype in the absence of the *lsy-6(ot150)* allele, with the exception of *F54D1.1* and *mxt-1*, whose depletion caused an occasional loss of *Plim-6::gfp* expression in ASEL (Figure 1B). Furthermore, RNAi of *T10E9.14*, *fubl-4, tofu-7* and *pno-1* resulted in variable and/or mild but not statistically significant enhancement of the *lsy-6(ot150)* phenotype (Figure 1B).

KH domain genes coordinate with *lsy-6* to regulate the expression of *cog-1*

Next, we wanted to determine whether the genes that genetically interacted with *lsy-6(ot150)* were also able to regulate a *lsy-6* target, *cog-1* (Johnston and Hobert 2003). Although *lsy-6* expression is normally restricted to neuronal tissues, its endogenous target *cog-1* is more broadly expressed (Palmer *et al.* 2002). Expression of *lsy-6* from the *cog-1* promoter represses the *cog-1::gfp* reporter in the uterine and vulval cells (Johnston and Hobert 2003) (Figure 2A). Therefore, we can use the *lsy-6*-mediated repression of *cog-1* to assay the effects of knocking down potential modulators of *lsy-6* activity. Indeed, RNAi of five genes, *sfa-1, tofu-7, pes-4, asd-2*, and *T10E9.14* resulted in a significant de-repression of *cog-1::gfp* expression in uterine cells (Figure 2B and Table 1), suggesting that these genes may coordinate with *lsy-6* in repressing *cog-1*. Although not statistically significant the knockdown of *tofu-7, asd-2, and F54DS1.1* mildly repressed *cog-1* expression in the uterine cells in the absence of *Pcog-1::lsy-6* (Figure 2B), suggesting these genes may regulate *cog-1* independently of *lsy-6*. In fact, *tofu-7, asd-2*, and *F54D1.1* may have a more complex functional relationship, perhaps regulating *cog-1* through multiple genetic pathways, including one that involves the *lsy-6* miRNA. Here, *tofu-7, asd-2*, and *F54D1.1* may act to promote *cog-1::gfp* expression in the absence of *lsy-6*, whereas the addition of *lsy-6* changes the functional relationship from positive to repressive or may deregulate target gene expression in either direction (Figure 2B).

KH domains proteins coordinate with *let-7* family of miRNAs

To determine whether KH domain-containing proteins might coordinate with additional miRNAs beyond *lsy-6*, we looked for a genetic interaction between the KH domain genes and the *let-7*-family of miRNAs. The *let-7* miRNA family, as part of a complex genetic network, regulates division patterns and terminal cell differentiation of seam cells during *C. elegans* larval development (Reinhart *et al.* 2000; Slack *et al.* 2000; Abbott *et al.* 2005). Three members of the *let-7* family, *mir-48, mir-241*, and *mir-84* act redundantly to control seam cell divisions by inhibiting the proliferative divisions of the L2 stage and promoting the self-renewing seam cell divisions of the L3 stage (Abbott *et al.* 2005). Loss of *mir-48, mir-241*, and *mir-84* leads to a highly penetrant reiteration of the proliferative L2 seam cell division leading to increased seam cell number, delayed alae formation, and delayed expression of the adult specific reporter, *col-19::gfp* (Abbott *et al.* 2005). Deletion of *mir-48* and *mir-241*, which leaves *mir-84* intact, results in milder heterochronic phenotypes including increased seam cell number and delayed alae formation (Abbott *et al.* 2005).

We performed RNAi for the twenty-four KH domain genes in the *mir-48 mir-241(nDf51)* mutant background and assayed both *col-19::gfp* expression and seam cell number in young adult animals (Figure 3, A and B). *mir-48 mir-241(nDf51)* young adults fail to properly undergo the adult-specific developmental program, thereby showing a delay in *col-19::gfp* expression consistent with a delay in normal developmental timing. RNAi of thirteen KH

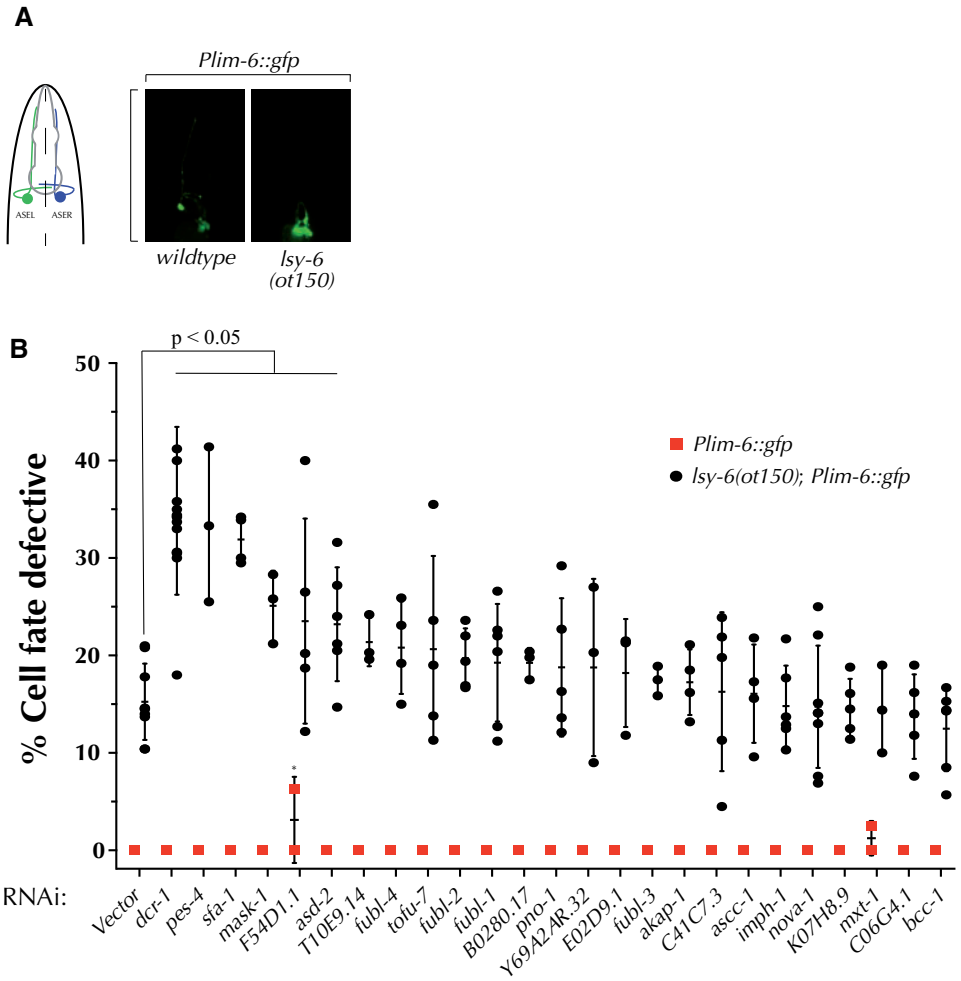

Figure 1 Knockdown of several KH domain genes enhances the cell defective phenotype of *lsy-6(ot150)* mutants. (A) *lsy-6* miRNA directs the ASEL cell fate specification, with ASEL cell fate marked by the *lim-6::gfp* reporter. *lsy-6(ot150)* mutations results in partially penetrant loss of *lim-6::gfp* expression in ASEL cells. (B) RNAi-mediated knockdown of five KH domain genes significantly enhances the cell fate defective phenotype of *lsy-6(ot150)* animals. ANOVA test was used to determine statistical significance.

domain genes significantly enhanced the abnormal *col-19::gfp* expression phenotype observed in *mir-48 mir-241(nDf51)* animals (Figure 3B and Table 1). RNAi of the twenty-four genes did not produce a phenotype in the absence of the *mir-48 mir-241* deletion (Figure 3B), with the exception of *B0280.17* RNAi, which showed a very mild defect in hypodermal *col-19::gfp* expression. In addition, *F54D1.1* RNAi produced a mildly penetrant abnormal *col-19::gfp* expression, but did not enhance the *mir-48 mir-241* phenotype to a statistically significant level (Figure 3B). RNAi of nine KH domain genes produced a significant increase in the average number of seam cells in the *mir-48 mir-241(nDf51)* mutants compared to the empty vector control (Figure 3C and Table 1). Overall, depletion of seven genes both enhanced the delayed hypodermal *col-19::gfp* expression and increased the seam cell number of *mir-48 mir-241(nDf51)* mutants (Figure 3, B and C, and Table 1). Together these data suggest that a subset of KH domain genes may coordinate, directly or indirectly, with the *let-7 family* miRNAs to regulate their target gene expression.

To further explore this level of coordination, we examined the role of KH domain genes in the regulation of *hbl-1*, a transcription factor and a known target of the *let-7* family of miRNAs (Abrahante *et al.* 2003; Lin *et al.* 2003; Abbott *et al.* 2005). Expression of *hbl-1* is normally temporally restricted to embryo-L2 animals and upon exit from the L2/L3 molt the expression of *hbl-1* is greatly reduced (Abbott *et al.* 2005). To understand how KH domain genes may be effecting *hbl-1* expression, either through the *let-7* family of miRNAs or independently, we performed RNAi of the top ten genes identified in the *mir-48 mir-241* assays as well as *F54D1.1* and assessed *hbl-1::gfp* expression. Normally, hypodermal *hbl-1::gfp* becomes downregulated as the animals molt from L2 to L3 and is largely absent in L3 animals (Figure 4A). Since reduction of miRNA activity results in inappropriate hypodermal *hbl-1* expression at the L3 stage, we sought to determine the percentage of worms displaying abnormal hypodermal *hbl-1::gfp* expression in early/mid L3 animals (Figure 4B). RNAi of *asd-2*, *C41G7.3*, and *sfa-1* produced a significant change in the abnormal expression of *hbl-1::gfp* in L3 animals, although most genes tested increased the abnormal expression in some RNAi replicates (Figure 4B). These data suggest that KH domain genes may play a role in the regulation of *hbl-1*, perhaps through the *let-7* family of miRNAs or through another indirect mechanism.

To assess the functional relevance of KH domain genes to miRNA activity later in development, we asked whether reducing KH domain gene function impacts activity of *let-7* itself. *let-7* governs the terminal seam cell differentiation during the transition

Table 1 KH domain genes functionally interact with miRNA sensitized mutants

Gene or allele	*lsy-6(ot150)*	*lsy-6*	*mir-48 mir-241(nDf51)*		*let-7(n2853)*	*alg-1(ma202)*
Assay RNAi	Cell fate[a] defective	Uterine[b] *cog-1::gfp*	Abnormal[c] *col-19::gfp*	Seam[d] Cell number	Bursting[e]	Wildtype[f] *col-19::gfp*
Empty vector	15.2 ± 3.9	48.8 ± 1.5	11.2 ± 7.9	13.4 ± 1.4	13.7 ± 6.9	0
dcr-1	34.9 ± 8.6	60.2 ± 10.8	79.4 ± 15.7	14.6 ± 1.9	33.4 ± 4.8	n.d.
fubl-3	17.4 ± 1.5	n.d.[g]	**50.4 ± 19.2**[h]	**14.2 ± 1.7**	**31.7 ± 8.7**	0
fubl-4	20.8 ± 4.7	46.6 ± 17.7	**49.7 ± 7.5**	14.1 ± 2.1	14.5 ± 10.6	0
fubl-1	19.3 ± 6.0	n.d.	**37.2 ± 29.5**	13.3 ± 1.4	24.2 ± 6.2	2.7 ± 3.8
fubl-2	19.7 ± 3.1	n.d.	22.3 ± 19.7	13.2 ± 1.5	12.2 ± 2.5	2.3 ± 3.2
imph-1	14.8 ± 4.2	n.d.	6.2 ± 5.4	13.5 ± 1.5	9.5 ± 1.8	7.3 ± 7.2
pes-4	**33.4 ± 8.0**	**66.2 ± 7.4**	**34.0 ± 12.2**	12.7 ± 1.1	10.6 ± 2.1	0
T10E9.14	21.4 ± 2.5	**63.9 ± 3.9**	**51.9 ± 18.9**	**14.1 ± 1.9**	15.9 ± 8.3	0
nova-1	14.7 ± 6.3	n.d.	6.7 ± 9.4	14.0 ± 1.6	11.5 ± 4.8	3.0 ± 4.2
mxt-1	14.5 ± 4.5	n.d.	26.6 ± 14.7	**14.2 ± 1.9**	**28.4 ± 11.9**	0
ascc-1	16.1 ± 5.1	n.d.	18.1 ± 13.5	13.2 ± 1.3	15.2 ± 7.1	4.2 ± 5.9
akap-1	17.3 ± 3.4	n.d.	**35.8 ± 2.1**	**14.1 ± 1.5**	13.2 ± 9.4	7.2 ± 10.1
tofu-7	20.6 ± 9.6	**71.6 ± 1.1**	**37.2 ± 18.2**	**14.2 ± 2.1**	17.5 ± 6.5	0
C06G4.1	13.7 ± 4.3	n.d.	13.9 ± 4.0	13.4 ± 1.6	10.9 ± 6.9	2.3 ± 3.2
E02D9.1	18.2 ± 5.5	n.d.	3.9 ± 6.8	13.2 ± 1.2	7.2 ± 5.4	**58.0 ± 19.0**
sfa-1	**32.0 ± 2.5**	**73.0 ± 9.0**	**43.9 ± 27.3**	**14.4 ± 1.8**	**25.3 ± 19.2**	7.2 ± 6.2
asd-2	**23.2 ± 5.8**	**65.4 ± 1.7**	**51.8 ± 23.9**	13.9 ± 1.9	**30.6 ± 19.8**	0
B0280.17	19.3 ± 1.5	n.d.	29.9 ± 19.8	13.5 ± 1.5	**31.5 ± 9.2**	0
F54D1.1	**23.5 ± 10.5**	58.3 ± 25.1	24.9 ± 7.7	13.9 ± 1.4	15.7 ± 7.0	0
K07H8.9	14.7 ± 2.9	n.d.	10.8 ± 14.3	13.7 ± 1.4	9.7 ± 5.4	3.0 ± 4.1
Y69A2AR.32	18.8 ± 9.1	n.d.	**40.8 ± 4.6**	13.5 ± 1.4	12.1 ± 3.0	6.0 ± 1.6
bcc-1	12.5 ± 4.4	n.d.	20.1 ± 12.5	**14.0 ± 1.9**	**31.0 ± 12.5**	0
C41G7.3	16.3 ± 8.2	n.d.	**45.5 ± 15.4**	**15.0 ± 2.3**	13.3 ± 9.2	1.4 ± 2.5
pno-1	18.8 ± 7.1	n.d.	**40.2 ± 12.0**	13.3 ± 1.4	14.0 ± 6.8	0
mask-1	**25.1 ± 3.6**	60.6 ± 5.8	**50.7 ± 18.6**	**14.7 ± 2.3**	12.9 ± 3.0	0

[a] *Plim-6::gfp* was scored in L4-Adult worms; $n > 160$ (range 160–965).
[b] Top enhancers of *lsy-6* activity were scored for uterine *cog-1::gfp* expression in L4 worms; $n > 36$ (range 36–106).
[c] *col-19::gfp* was scored in young adult worms; $n > 25$ (range 25–186).
[d] Seam cell number was scored at the same time as *col-19::GFP* expression in young adults; $n > 25$ (range 25–186).
[e] Synchronized L1 worms were reared at 15°C; vulval bursting scored in day 1 adults; $n > 98$ (range 98-364).
[f] *col-19::gfp* was scored in young adult worms; $n > 18$ (range 18–40).
[g] n.d. - not determined.
[h] Values showing statistical significance are shown in bold.

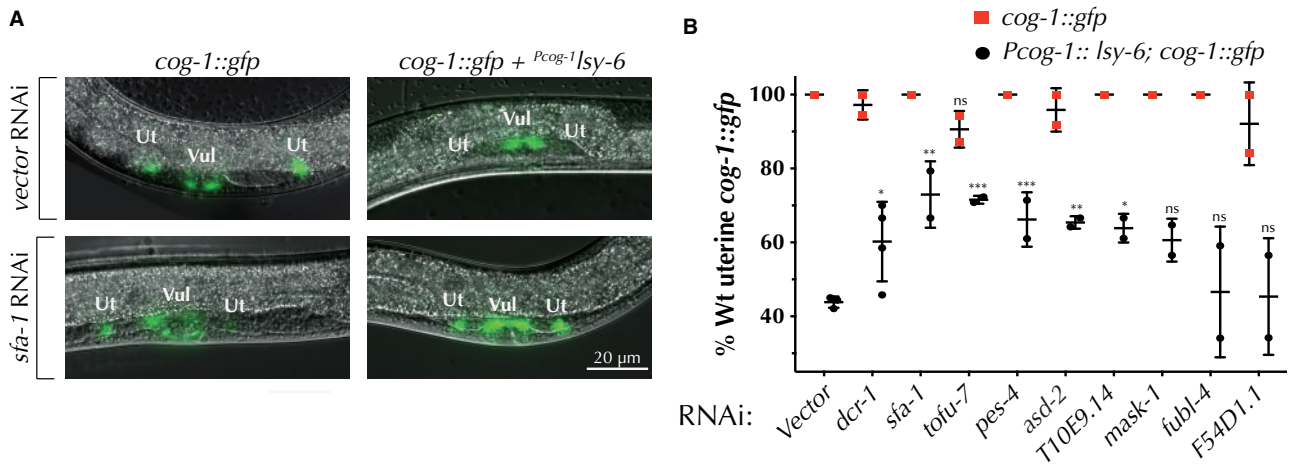

Figure 2 Several KH domain genes coordinate with *lsy-6* to regulate *cog-1::gfp* expression in uterine cells. (A) RNAi of several KH domain genes, including *sfa-1* alleviates the *lsy-6*-mediated repression of *cog-1::gfp* in uterine cells (B). ANOVA test was used to determine statistical significance. $^{*}P \leq 0.05$, $^{**}P \leq 0.01$, $^{***}P \leq 0.001$.

from L4 to adulthood (Reinhart *et al.* 2000). Compromising *let-7* miRNA activity produces a heterochronic phenotype, which, among other defects, includes vulval rupture during the L4-adult molt (Reinhart *et al.* 2000). *let-7(n2853)*, a temperature sensitive reduction-of-function mutation, causes a mildly penetrant vulval rupture phenotype at 15°C (Figure 5A) (Reinhart *et al.* 2000). RNAi of six KH domain genes led to significant enhancement of the vuval bursting phenotype (Figure 5B) suggesting these genes may coordinate with *let-7* miRNA in a way that normally promotes its activity.

To further explore the genetic interaction between KH domain genes and *let-7* miRNA, we asked whether KH domain genes can regulate expression of a *let-7* target, *lin-41* (Vella *et al.* 2004). We performed RNAi of four of the genes identified in the *let-7(n2853)* assay, using three reporter strains: *Pdpy-30::gfp::lin-41 3′UTR*

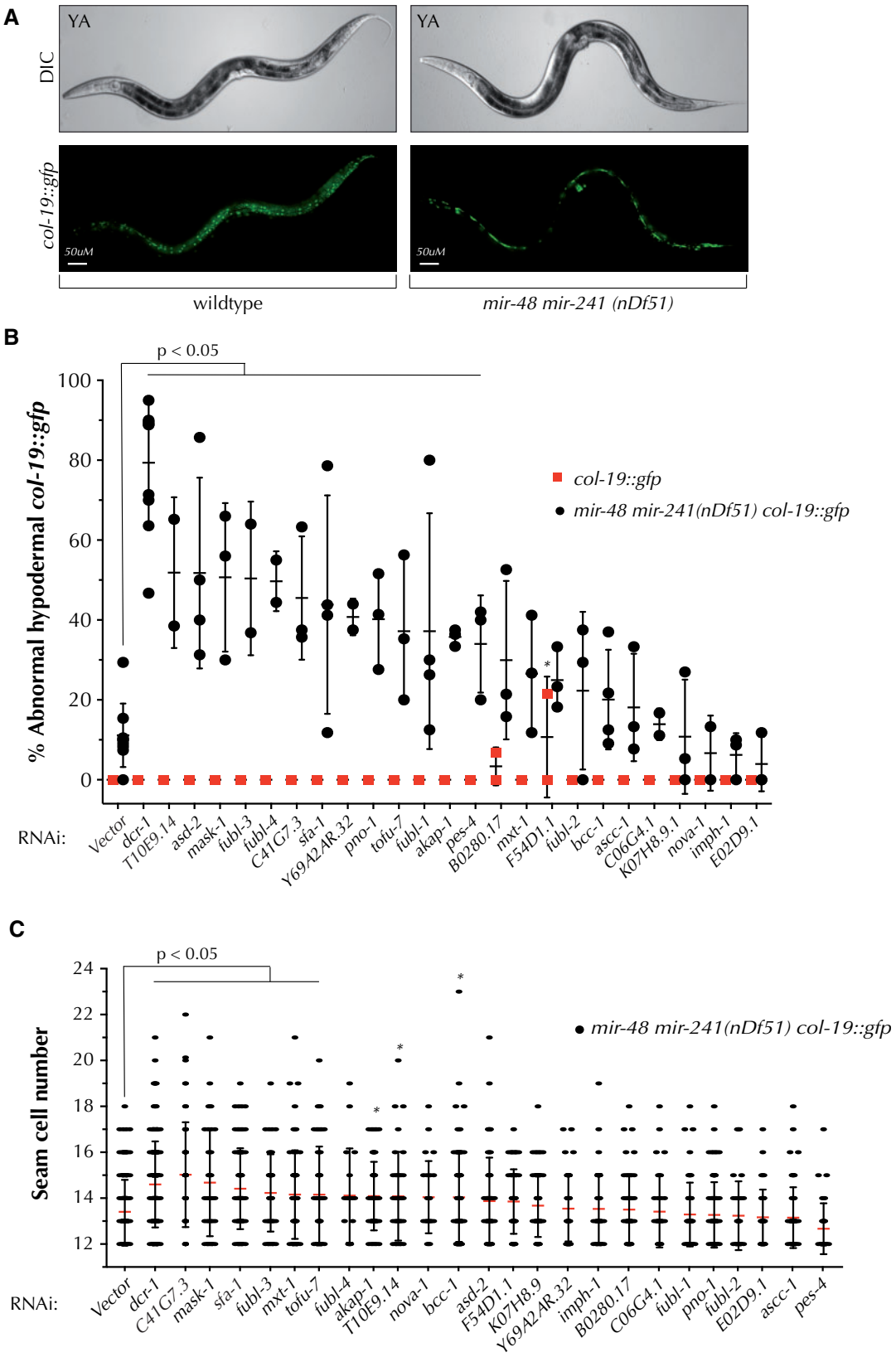

Figure 3 RNAi of multiple KH domain genes enhances the *mir-48 mir-241* heterochronic phenotype. (A) Loss of *mir-48 mir-241* results in delayed hypodermal expression of the adult specific marker *col-19::gfp*. (B) When compared to vector RNAi, knockdown of 13 KH domain genes by RNAi enhances the delayed hypodermal *col-19::gfp* expression of *mir-48 mir-241(nDf51)* animals. Dots represent experimental replicates. (C) RNAi of some KH domain genes increases the seam cell numbers of *mir-48 mir-241(nDf51)* young adults when compared to vector RNAi. ANOVA test was used to determine statistical significance. *$P \leq 0.05$

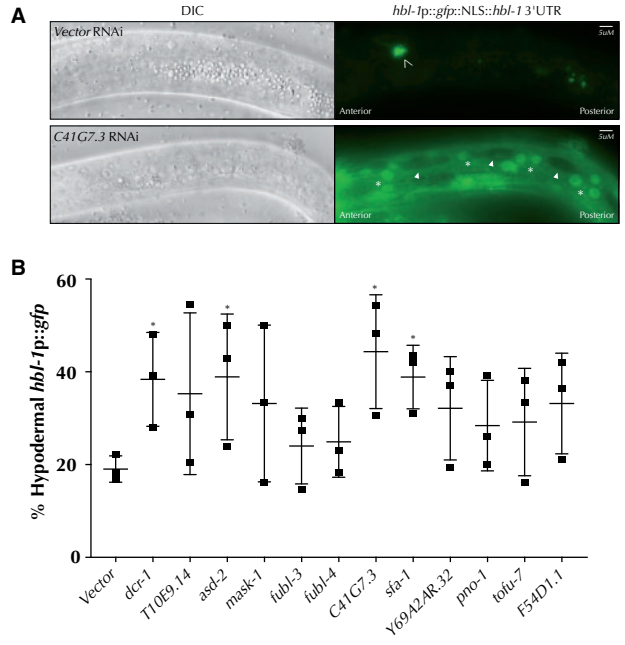

Figure 4 RNAi of some KH domain genes affect *hbl-1::gfp* expression. (A) *hbl-1::gfp::hbl-1* 3′ UTR expression in vector RNAi control and C41G7.3 RNAi L3 larvae. (B) RNAi of C41G7.3 and other KH domain genes significantly enhances the number of animals displaying hypodermal expression of *hbl-1::gfp::hbl-1* 3′ UTR in L3 animals. Hypodermal cells are labeled with white asterisks. Seam cell nuclei are labeled with white arrowheads. Non-hypodermal neuron is indicated with an open arrowhead. ANOVA test was used to determine statistical significance. $^{*}P \leq 0.05$.

alone, *Pdpy-30::gfp::lin-41 3′UTR* with *let-7(n2853)*, and *Pdpy-30::gfp::lin-41 3′UTR* delta LCS (two major *let-7* binding sites removed from the *lin-41* 3′UTR) (Ecsedi *et al.* 2015). These strains also express an *Pdpy-30*::mCherry control reporter with a synthetic 3′UTR, which provides a convenient tool to quantify *let-7* activity via GFP expression (Figure 5C; Ecsedi *et al.* 2015). RNAi of each *B0280.17* and *mxt-1* de-repressed *GFP::lin-41 3′UTR* (Figure 5, C and D). RNAi of the *B0280.17*, *asd-2*, *mxt-1*, and *sfa-1* significantly de-repressed *GFP::lin-41 3′UTR* when *let-7* function was compromised (Figure 5, C and D). However, *asd-2*, *mxt-1*, and *sfa-1* also significantly de-repressed *GFP::lin-41* delta LCS *3′UTR* (Figure 5D), indicating that these effects on *lin-41::gfp* are not directed through the two *let-7* sites deleted in this reporter strain, at least not exclusively. Interestingly, RNAi of *dcr-1* also increased the *lin-41::gfp* fluorescence level both in the *lin-41::gfp; let-7(n2853)* and *lin-41::gfp delta LCS* backgrounds (Figure 5D), suggesting that other miRNA target sites might be engaged in regulation of *lin-41::gfp*. These data support the possibility that *B0280.17* may be coordinating with *let-7* miRNA to regulate *lin-41::gfp*, whereas other genes may also regulate *lin-41::gfp* independently of *let-7* under these conditions.

Knockdown of KH domain genes suppresses compromised miRISC activity

ALG-1 is one of two *C. elegans* Argonautes (ALG-1 and ALG-2) that primarily associate with miRNAs and are central for miRNA biogenesis and activity (Grishok *et al.* 2005). Mutations abolishing ALG-1 activity result in moderate developmental defects, whereas abolishing both *alg-1* and *alg-2* activity results in early lethality (Grishok *et al.* 2005; Vasquez-Rifo *et al.* 2012). In addition, antimorphic mutations in *alg-1*, such as *alg-1(ma202)*, result in more pronounced defects in miRNA activity, likely due to sequestration of miRNA pathway components away from ALG-2 (Zinovyeva *et al.* 2014). Specifically, *alg-1(ma202)* animals display severe heterochronic defects (Zinovyeva *et al.* 2014), with 100% of *alg-1(ma202)* young adult animals failing to appropriately express adult cell marker *col-19::gfp* in hyp7 hypodermal cells (Zinovyeva *et al.* 2014) (Figure 6, A and B). Expression of *col-19::gfp* in young adult seam cells of *alg-1(ma202)* is variable, ranging from a complete lack of expression in the seam cells to full seam cell expression (Zinovyeva *et al.* 2014).

To determine whether any of the KH domain genes might normally have a negative genetic relationship with miRNA pathway components, we performed RNAi knockdown of KH domain genes in the *alg-1(ma202)* background and assessed *col-19::gfp* expression in hypodermal cells of young adult animals. We used this background to screen for genes that may normally negatively interact with the miRNA pathways and therefore suppress the *alg-1(ma202)* phenotype when knocked down. Interestingly, RNAi of *E02D9.1* significantly suppressed the abnormal hypodermal *col-19::gfp* expression in *alg-1(ma202)* young adults, with ~60% of *alg-1(ma202)* animals showing wild type hypodermal *col-19::gfp* expression in young adults (Figure 6, A and B, and Table 1). Although not statistically significant, possibly due to the variation in RNAi efficiency, RNAi of other genes (most notably *imph-1*, *sfa-1*, *akap-1*, and Y69A2AR.32) restored wild type *col-19::gfp* expression in *alg-1(ma202)* young adults, something that is never observed in *alg-1(ma202)* mutants alone (Figure 6B). As *alg-1(ma202)* suppressors, these KH domain genes may act in a manner that opposes normal miRNA activity, with their depletion perhaps resulting in decreased miRNA target gene expression.

KH domain containing RBPs play a role in early development

To determine whether KH domain genes have a general effect on *C. elegans* development, we assayed the brood size and embryonic lethality of animals with reduced KH domain gene function. Knockdown of seven genes (*fubl-4*, *pes-4*, *akap-1*, *E02D9.1*, *sfa-1*, *Y69A2AR.32*, and *bcc-1*) resulted in significant reduction in brood size (Figure 7A and Table 2), Depletion of *sfa-1* and *pes-4* had significant effects on both brood size and embryonic lethality suggesting that these genes play fundamental roles in *C. elegans* development (Figure 7, A and B, and Table 2). Several additional genes disrupted early development, albeit to a degree that was not statistically significantly by our analysis (Figure 7 and Table 2). These observations are consistent with previously reported roles for *akap-1*, *E02D9.1*, *sfa-1*, *asd-2*, *K07H8.9*, and *bcc-1* in early *C. elegans* development (Kamath *et al.* 2003; Sönnichsen *et al.* 2005; Ohno *et al.* 2008; Ma and Horvitz 2009; Kapelle and Reinke 2011) and highlight additional genes as important for *C. elegans* fecundity and embryonic development.

Some *C. elegans* KH domain proteins are evolutionary related and have diverse domain architecture

Protein domains are discrete functional and structural segments of a protein. The loss, gain, or structural modification of domains can drive evolution, allowing proteins to lose or acquire new functions over evolutionary time. As domains evolve from ancestral forms, proteins containing the same types of domains may be evolutionary related. To understand the evolutionary relationship between the KH domain-containing proteins and to potentially inform our functional analysis, we performed an alignment of *C. elegans* KH domain protein sequences using the MEGAx

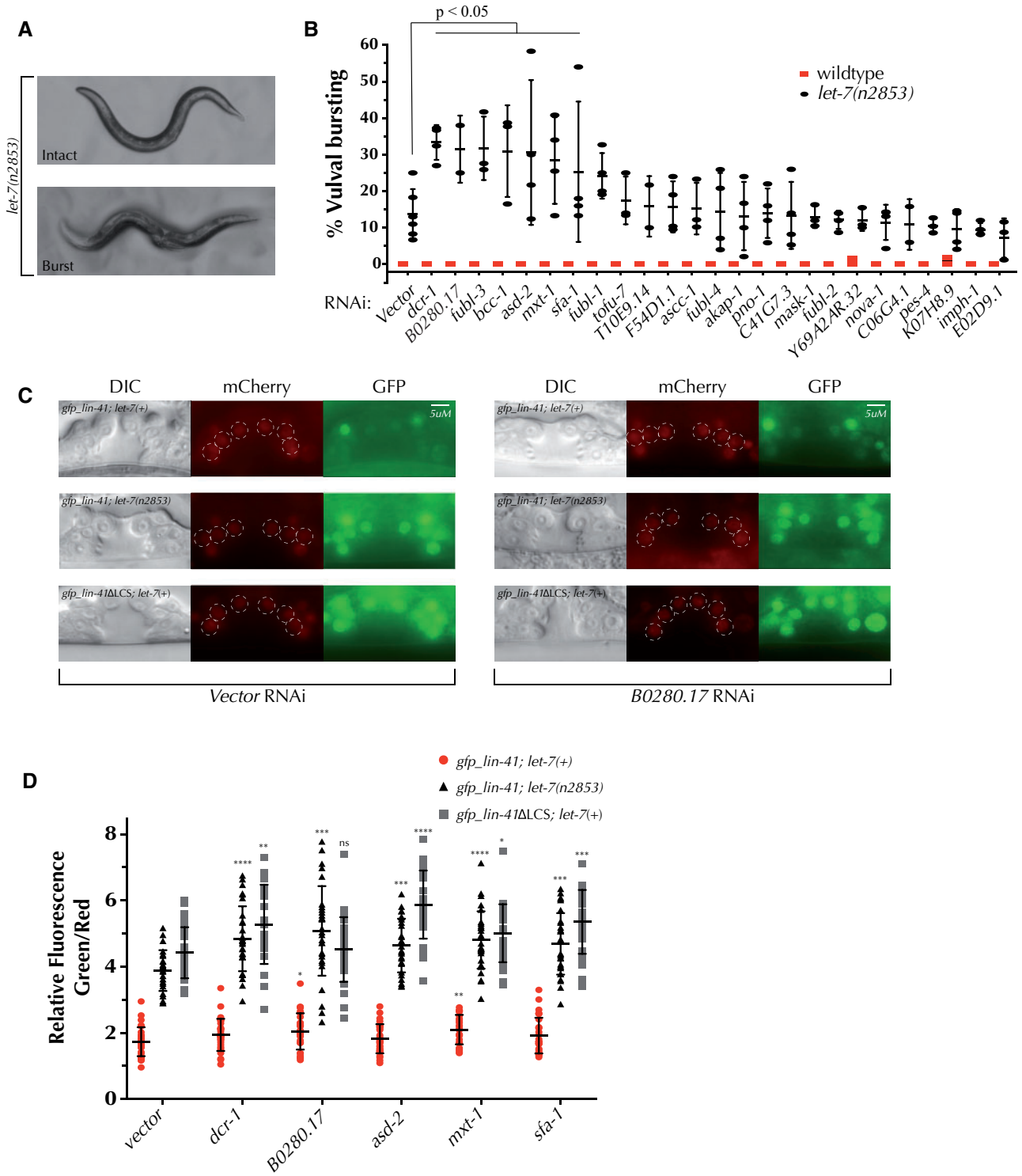

Figure 5 Several KH domain genes interact genetically with the *let-7* miRNA and its target *lin-41*. (A, B) *let-5(n2853)* worms display a partially penetrant vulval bursting phenotype at permissive temperature (15 °C). (B) RNAi knockdown of six KH domain genes significantly enhances the vulval bursting phenotype of *let-7(n2853)* worms. (C) Expression of a reporter system previously designed to assess miRNA activity on miRNA target *lin-41* 3′ UTR (Ecsedi *et al.* 2015) in vector control and B0280.17 RNAi. Three strains express *Pdpy-30::GFP::lin-41* 3′UTR and *Pdpy-30::mCherry* control in vulval cells: wild type (*gfp_lin-41; let-7(+)*), *let-7(n2853)* (*gfp_lin-41; let-4(n2853)*), and wild type *let-7* with *lin-41ΔLCS* reporter lacking the two functional *let-7* complementary sites within the *lin-41* 3′UTR (*gfp_lin-41ΔLCS; let-7(+)*). When *let-7* activity is compromised or *let-7* sites are removed from *lin-41* 3′UTR, *GFP* expression is de-repressed (quantified in D). (D) RNAi of 4 KH domain genes alleviates the repression on *GFP::lin-41 3′UTR* expression when *let-7* activity is compromised. Images shown in (C) were adjusted post-quantification to allow reader to more easily visualize vulval cells. Cells quantified are highlighted with dashed circles. ANOVA test was used to determine statistical significance. *$P \leq 0.05$, **$P \leq 0.01$, ***$P \leq 0.001$, ****$P < 0.0001$.

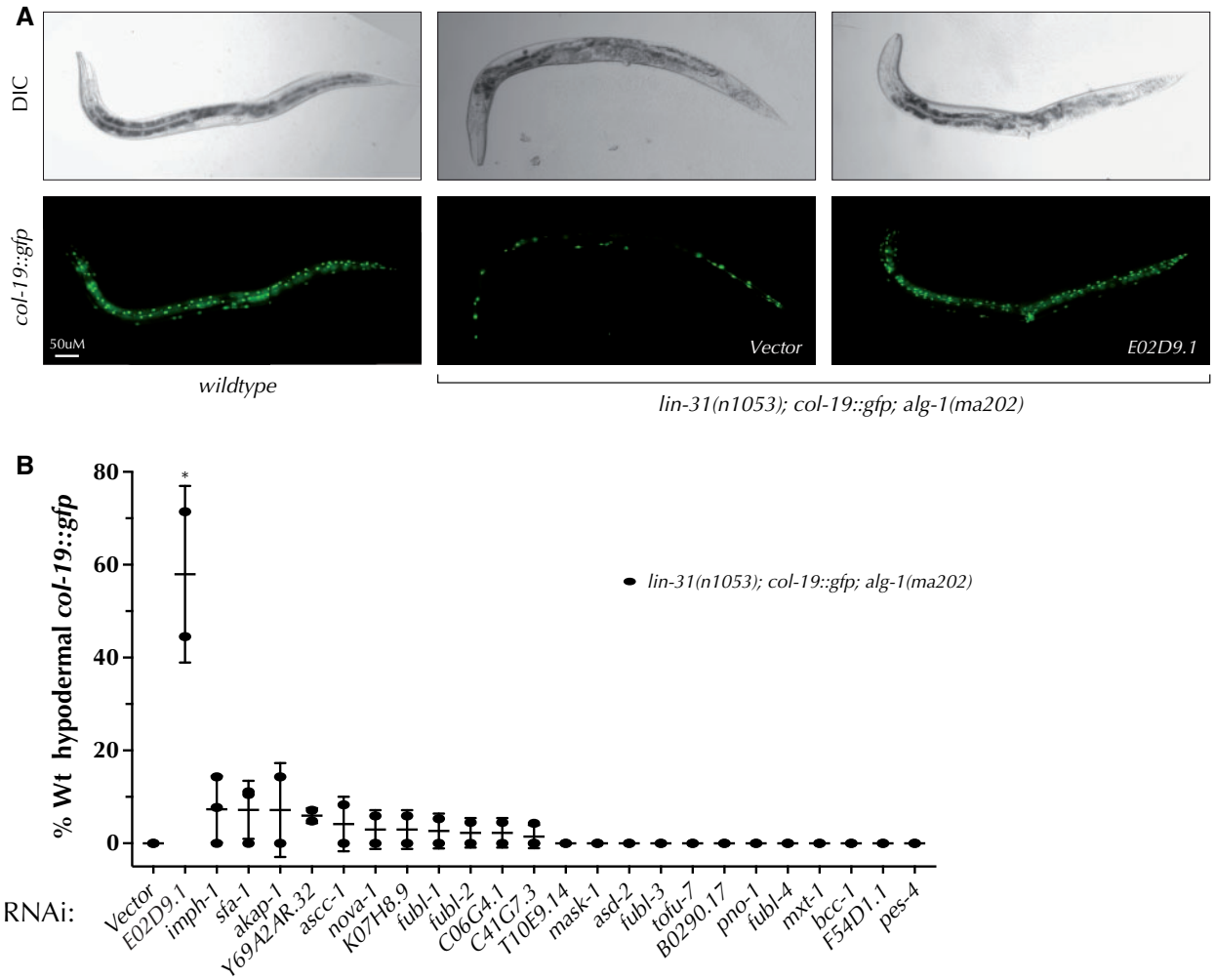

Figure 6 Two KH domain containing genes interact genetically with ALG-1(*ma202*). (A) *alg-1(ma202)* young adults lack hypodermal *col-19::gfp* expression and display variable *col-19::gfp* expression in seam cells. The *alg-1(ma202)* mutation is present in a *lin-31(n1053)* background to suppress bursting via non-heterochronic mechanisms. RNAi of *E02D9.1* restores *col-19::gfp* expression in young adults (A, B). (B) RNAi of several genes suppresses the delayed *col-19::gfp* expression phenotype of *alg-1(ma202)* mutants. ANOVA test was used to determine statistical significance. $^{*}P \leq 0.05$.

alignment program (Kumar *et al.* 2018) and generated a phylogenetic tree (Figure 8). Interestingly, proteins that appear to coordinate with miRNAs are found in almost every clade in our phylogenetic analysis (Figure 8).

KH domains are thought to mediate numerous interactions, including those between proteins (Valverde *et al.* 2008) and proteins and nucleic acids (Grishin 2001; Valverde *et al.* 2008). Due to the KH domain's ability to bind RNA, the *C. elegans* KH domain-containing proteins represent a subset of RBPs, but combinatorial domain arrangements can result in extensive functional diversity among them. To determine the diversity of domain structures of KH domain containing proteins, we analyzed their domain architecture using the Simple Modular Architecture Research Tool (SMART) (Letunic and Bork 2017), which identifies known domain sequences. In addition, we used the PLACC web-based tool to identify prion-like domains, or unstructured regions (Lancaster *et al.* 2014). Such low complexity regions are thought to have affinity for RNA (Kato *et al.* 2012) and can play a role in phase-phase separation that is important for forming and reforming of ribonucleoprotein (RNP) bodies (Shin and Brangwynne 2017). We found that KH domain-containing proteins harbor a diverse set of domains, with prion-like domains present in 17/29 of KH domain proteins (Figure 9). Unsurprisingly, many proteins of the same clade shared additional domains (Figures 8 and 9). These analyses may in the future help inform the mechanisms by which these proteins coordinate with miRNA-mediated regulation of gene expression.

Discussion

KH-domain containing RBPs functionally interact with multiple miRNA families

To determine whether *C. elegans* KH domain-containing RBPs may function with miRNAs to regulate gene expression, we asked whether RNAi knockdown of KH domain genes could modify the phenotypes observed in reduction-of-function miRNA or family mutants. Surprisingly, eighteen of the twenty-four tested genes genetically interacted with at least one miRNA mutant background, suggesting widespread functional interaction between KH RBPs and miRNAs. Interestingly, the KH domain genes fell into two groups: those that modified phenotypes of all miRNA sensitized backgrounds tested and those that genetically interacted with specific miRNA reduction-of-function mutants (Table 1). *sfa-1 and asd-2* functionally interacted with multiple miRNA families (Table 1), suggesting that these two genes have broad roles in regulation of gene expression. The human ortholog

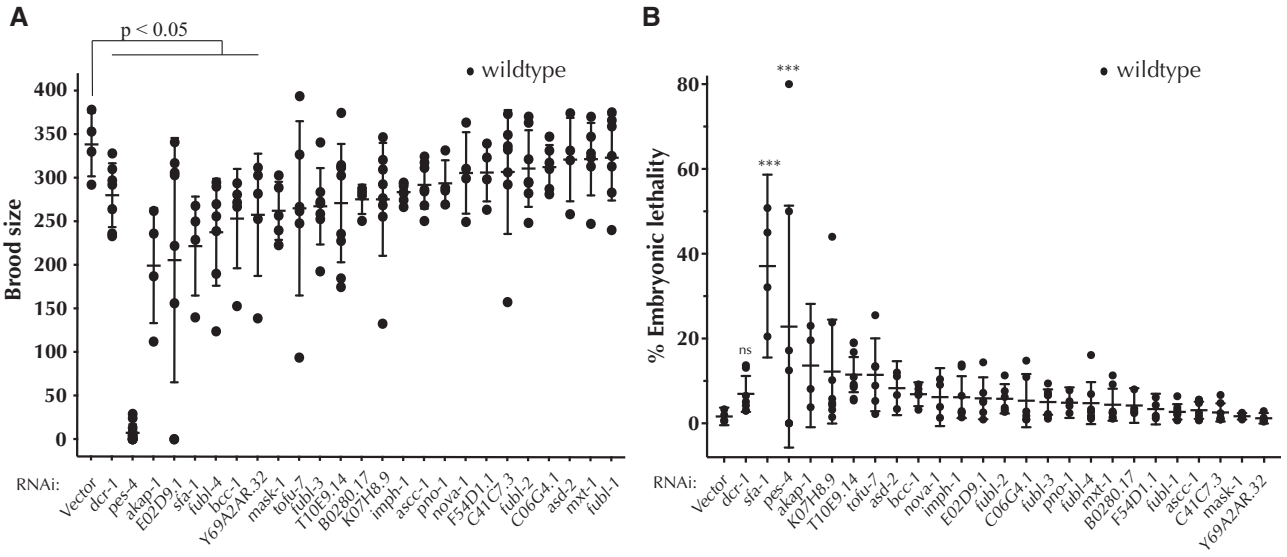

Figure 7 KH domain containing RNA-binding proteins may have essential roles in development. (A) RNAi of seven KH domain genes resulted in significant reductions in brood size. (B) After knockdown *sfa-1* and *pes-4* significantly enhance embryonic lethality. ANOVA test was used to determine statistical significance. $^{***}P \leq 0.001$.

Table 2 Knockdown of KH domain genes affects embryonic lethality and brood size

Assay RNAi	% Embryonic *a* lethality (n)	Brood size *b*
Empty vector	1.6 ± 1.3 (4)	338.3 ± 36.5
dcr-1	6.9 ± 4.6 (7)	280.0 ± 36.6
fubl-3	5.0 ± 3.3(7)	267.7 ± 43.9
fubl-4	4.8 ± 5.4 (7)	237.7 ± 61.4
fubl-1	2.1 ± 2.0 (7)	324.0 ± 49.1
fubl-2	5.8 ± 3.3 (6)	311.4 ± 44.1
imph-1	6.2 ± 5.4 (7)	284.1 ± 10.3
pes-4	22.8 ± 30.9 (7)	7.2 ± 9.9
T10E9.14	11.5 ± 5.4 (9)	271.3 ± 67.9
nova-1	6.2 ± 4.3 (4)	306.3 ± 46.8
mxt-1	4.4 ± 4.1 (7)	322.3 ± 41.6
ascc-1	3.1 ± 2.2 (7)	292.4 ± 27.2
akap-1	13.6 ± 9.1 (4)	199.3 ± 66.0
tofu-7	11.5 ± 8.2 (6)	265.3 ± 100.0
C06G4.1	5.4 ± 6.0 (6)	313.2 ± 25.3
E02D9.1	5.9 ± 6.0 (6)	205.6 ± 140.2
sfa-1	37.1 ± 13.6 (4)	221.8 ± 56.8
asd-2	8.3 ± 4.0 (4)	321.8 ± 47.9
B0280.17	4.2 ± 2.6 (4)	275.8 ± 16.8
F54D1.1	3.4 ± 2.7 (4)	306.8 ± 33.1
K07H8.9	12.2 ± 14.7 (8)	275.8 ± 64.8
Y69A2AR.32	1.2 ± 1.0 (5)	257.8 ± 70.2
bcc-1	6.9 ± 2.3 (5)	253.4 ± 57.1
C41G7.3	2.6 ± 2.3 (7)	307.4 ± 71.1
pno-1	4.9 ± 2.3 (4)	294.3 ± 26.5
mask-1	1.7 ± 0.6 (5)	262.4 ± 33.3

[a] All worms were grown at 20°C; dead embryos were counted 1 day after being laid; n = number of broods; $n > 4$ (range 4–9).
[b] All worms were grown at 20°C; brood size includes dead embryos, arrested larvae and living progeny; n = number of broods; $n > 4$ (range 4–9).

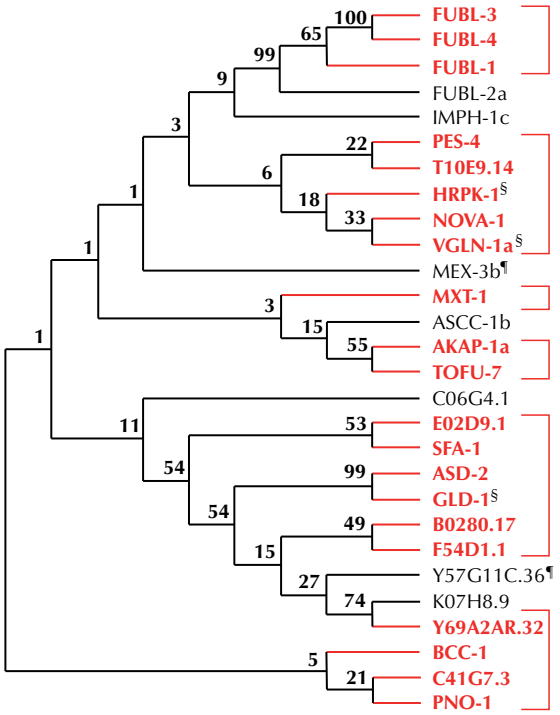

Figure 8 Phylogenetic analysis of KH domain containing RNA-binding proteins. Multiple sequence alignment of 28 KH domain containing RNA-binding proteins was performed and the proteins grouped in clades based on sequence similarity; branches are labeled with confidence value. Clades containing proteins that genetically interact with one or more miRNA sensitized background are bracketed and highlighted in red. A ¶ indicates that functional assays were not performed for a particular gene. A § denotes genes identified as interacting with miRNAs in other publications.

of *sfa-1*, SF1 (Splicing Factor 1), participates in the spliceosome assembly by binding 3′ branch sites of pre-mRNAs, whereas its partner, U2AF, cooperatively binds the 5′ branch site (Rino *et al.* 2008). Likewise, the ortholog of *asd-2*, *quaking*, has established roles in RNA processing, including alternative splicing and generation of select miRNAs and circular RNAs (Darbelli and Richard 2016). In *C. elegans*, both *sfa-1* and *asd-2* are predicted to play a role in splicing, with *asd-2* modulating the alternative splicing of *unc-60* and other transcripts (Kuroyanagi 2013) and *sfa-1* regulating the pre-mRNA splicing of multiple genes (Heintz *et al.* 2017). Depletion of either *sfa-1* or *asd-2* was sufficient to induce embryonic lethality and reduce brood sizes (Table 2) (Ma and Horvitz

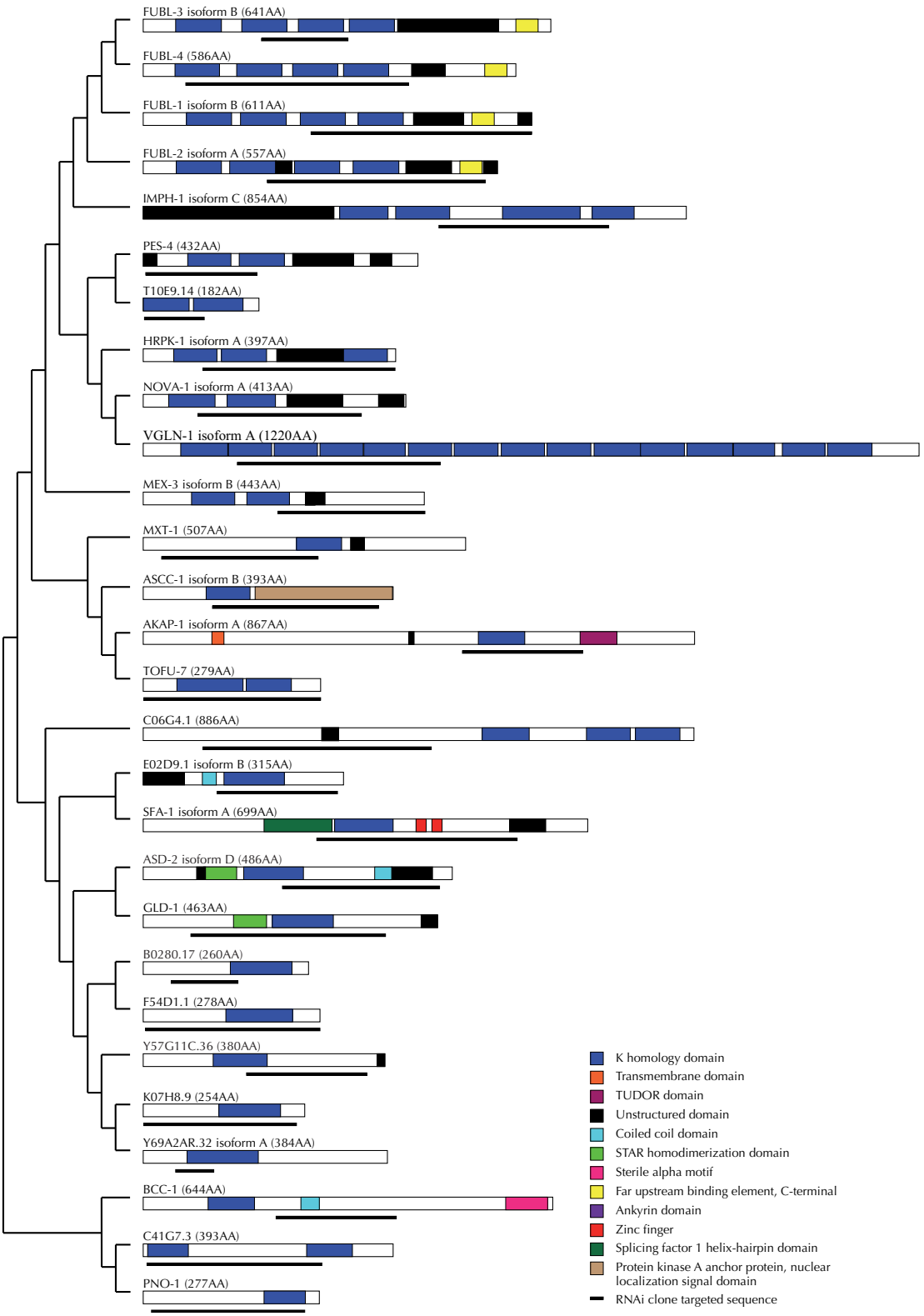

Figure 9 Domain architecture analysis of KH domain containing RNA-binding proteins. Protein domains prediction analysis was performed on the longest predicted isoform using SMART (Letunic and Bork 2017). Region of each protein targeted by RNAi are highlighted below the predicted protein structure. Proteins are grouped in the clades identified via our phylogenetic analysis.

2009; Chu *et al.* 2014), consistent with their essential roles as potential global regulators of splicing. Unbiased reverse genetic screens have previously identified splicing machinery members as important for miRNA-mediated gene regulations (Parry *et al.* 2007). Similarly, factors involved in mRNA processing, including splicing, were found to modulate RNAi efficacy (Kim *et al.* 2005).

Although splicing and small RNA (including miRNA) pathways intersect, the exact mechanisms by which this occurs remain largely unknown. Given *sfa-1* and *asd-2* potential roles in splicing, it is perhaps not surprising that these factors show broad genetic interaction with miRNAs across all of our assays.

To better understand the biological context in which miRNAs and KH domain proteins may interact, we compiled spatial KH domain gene expression patterns using existing promoterome (Hunt-Newbury *et al.* 2007), tissue-specific transcriptome (Kaletsky *et al.* 2018), and tissue-specific proteome (Reinke *et al.* 2017) datasets (Supplementary Table S3). Most KH domain genes are broadly expressed with both transcripts and proteins detected in multiple tissues (Supplementary Table S3). For the most part, genes whose RNAi produced a phenotype in a particular miRNA background seemed to be expressed in the relevant tissues. For example, Y69A2AR.32 expression in the hypodermis correlated with its knockdown effects on *col-19::gfp* expression in *mir-48 mir-241* mutant animals (Figure 3). Similarly, most of the KH domain genes whose knockdown resulted in *lsy-6(ot150)* phenotype enhancement are neuronally expressed, although it remains unknown whether these KH domain genes are specifically expressed in ASEL/R neurons. Future work is needed to characterize precise tissue and cellular expression to fully understand the spatial and temporal overlap among the molecules in question.

In contrast to the splicing-related factors, the majority of the KH domain-containing RBPs genetically interact with specific miRNAs (Table 1). RNAi knockdown of *pes-4* and *mask-1* enhances phenotypes of both *lsy-6(ot150)* (Figure 1 and Table 1) and *mir-48 mir-241(nDf51)* (Figure 3 and Table 1) mutants, suggesting a somewhat general role in gene regulation that spans multiple tissues. By contrast, *akap-1, C41G7.3, pno-1*, *fubl-1*, *fubl-4*, and *Y69A2AR.32* genetically interacted with *mir-48 mir-241(nDf51)* (Figure 3 and Table 1), but not *let-7(n2853)* (Figure 5 and Table 1), suggesting a narrower role for these KH domain genes in target gene regulation. Such functional separation can be achieved through differences in temporal expression or perhaps through distinct specificities of RBPs to target RNAs. In comparison, RNAi of *bcc-1*, *fubl-3* and *mxt-1* genetically interacted with both *mir-48 mir-241(nDf51)* and *let-7(n2853)*, but not *lsy-6(ot150)* (Table 1). The *let-7-family* shared interactions suggest that these RBPs may have more general roles in developmental timing or may regulate broader sets of target genes. Interestingly, *fubl-1 (C12D8.1)* was previously identified as a functional interactor of RNAi (Kim *et al.* 2005), suggesting that this gene's activity may impact gene regulation carried out by multiple small RNA pathways. *tofu-7* was previously identified in a screen for regulators of piRNA biogenesis and function (Goh *et al.* 2014). In addition, *fubl-1*, *fubl-3*, *fubl-4*, *imph-1*, and *nova-1* show significant phylogenetic clustering with RNAi related genes when integrating existing immunoprecipitation and *Drosophila* miRNA and siRNA datasets into cluster analysis (Tabach *et al.* 2013). Taken together, these observations suggest that some of the KH domain genes may coordinate with several small RNA pathways.

KH domain protein relatedness

Protein domains are conserved, structured portions of a protein that can fold and function independently. As distinct functional units of a protein, they can dictate, or add to, the overall cellular and molecular role of the protein. Evolution of protein structure and function is in part driven by addition or removal of domains through genetic recombination of domain-encoding gene sequences. To better understand the evolutionary and functional relatedness of the KH domain-containing proteins in *C. elegans* we performed a phylogenetic analysis (Figure 8). Our analysis highlights the overall diversity of these proteins, revealing low levels of similarity between many of the clades, consistent with the observation that in many cases, the proteins sequence similarity is limited to the KH domain(s). However, in contrast to the overall diversity of the proteins, we do see high degrees of relatedness in several of the clades, most notably those containing the FUBL proteins and the grouping consisting of GLD-1 and ASD-2 (Figure 8). This is not surprising given the similarity in domains and overall protein architecture (Figure 9). The phylogeny highlights several clades that genetically interact with miRNAs (Figure 8), perhaps reflecting the functional relatedness relevant to regulation of gene expression. We note that high degree of similarity between the *fubl* genes could have resulted in some cross-reactivity during RNAi knockdown. However, only RNAi knockdown against *fubl-3* elicited enhancement of the *let-7(n2853)* phenotype (Table 1), suggesting some specificity, at least in the case of *fubl-3* knock-down.

Potential models for KH domain RBP and miRNA coordination

How might KH domain RBPs functionally interact with miRNA pathways to regulate gene expression? Given the evolutionary and domain architecture diversity, the KH RBPs may coordinate with miRNAs, directly or indirectly, via distinct mechanisms. KH RBPs may directly affect aspects of miRNA biogenesis and function or they may indirectly intersect with miRNA pathways by affecting target mRNA processing, transport, stability, and degradation, independent of miRNA activity.

Overall, KH RBPs may exert their gene regulatory effects on miRNA targets indirectly, through multiple effectors (Figure 10A). Alternatively, KH RBPs could more directly regulate the life cycle of miRNA targets by interfacing directly with the miRNAs themselves or with the target mRNAs (Figure 10B). There are multiple mechanisms through which KH RBPs could contribute to miRNA target gene regulation. Proteins involved in splicing, such as SFA-1 and ASD-2, may be involved in splicing events that lead to the production of miRNA transcripts either from their independent gene loci or as part of host mRNA processing (Figure 10C). In this scenario, loss of a splicing factor's function may reduce the amount of primary miRNA transcript produced, enhancing the reduction of function phenotypes observed in our sensitized backgrounds (Figure 10C). In addition, splicing factors may indirectly intersect with miRNA pathways by either increasing or decreasing the availability of a gene target (Figure 10D). Alternative splicing of 3′ UTRs that eliminate miRNA target sites has been recently observed (Han *et al.* 2018). Under this model, KH domain gene depletion could result in alternatively spliced mRNA isoforms that are no longer able to escape miRNA-mediated regulation (Figure 10D), enhancing the phenotypes observed in our reduction of function miRNA mutants.

In another possible scenario, KH domain-containing factors may affect mRNA stability, localization, or transport and thus alter the pool of available miRNA targets (Figure 10E). Increased stability of target mRNAs perhaps through sequestration could reduce miRNA efficacy (Figure 10E). In contrast, reduced stability of miRNA target mRNAs could result in suppression of miRNA-related phenotypes observed in our assays. Interestingly, *Drosophila* orthologs of MXT-1 (MEXTLI) and B0280.17 (HOW) can enhance the stability of mRNAs (Nabel-Rosen *et al.* 2002; Hernández *et al.* 2013). The B0280.17 ortholog (HOW) shows isoform dependent enhancement or suppression of mRNA stability

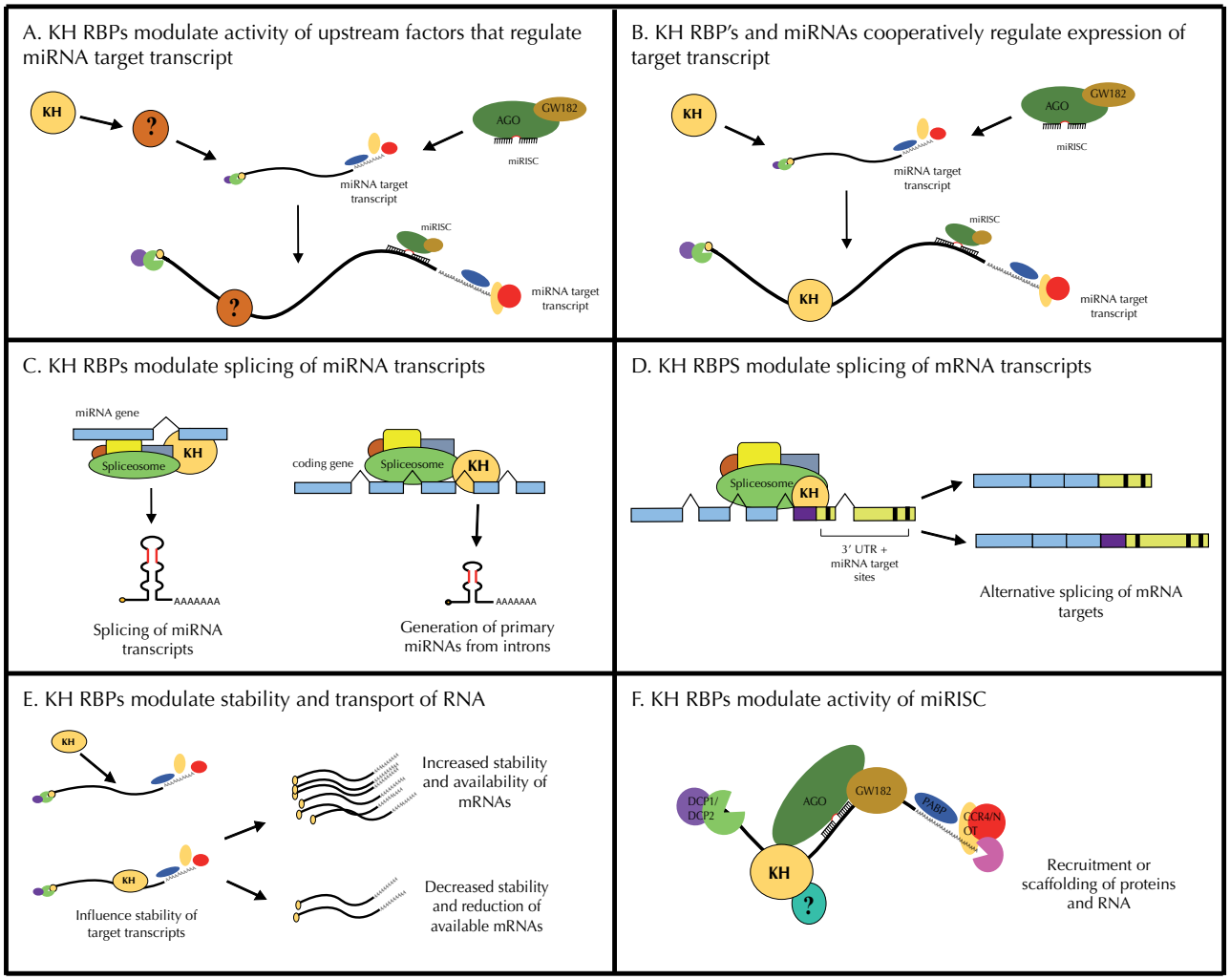

Figure 10 Models for potential interactions between miRNAs and KH domain-containing RNA binding proteins. (A) KH RBPs may indirectly modulate miRNA target gene expression through one or more intermediate effector(s). (B) KH RBPs may regulate miRNA target gene expression by acting directly on the miRNA target transcripts as elaborated on in C–F. (C) KH RBPs may modulate the splicing of primary miRNA transcripts. (D) RBPs may modulate the splicing of miRNA target transcripts and alter the availability of miRNA target sites in their 3′ UTRs. (E) RBPs may modulate the stability of miRNA target transcripts. Loss of KH domain proteins could increase the pool of target mRNAs, enhancing the miRNA reduction-of-function phenotypes, or decrease the pool of target mRNAs, resulting in the suppression of miRNA mutant phenotypes. (F) RBPs may modulate the activity of miRISC by bridging known RNA and protein components or by the recruitment of additional regulatory factors.

in order to modulate mRNA translation (Hernández *et al.* 2013). Likewise, the human orthologs of the FUBL proteins can positively or negatively modulate (depending on the protein) translation of their mRNA targets by binding the 3′ UTRs and influencing their stability (Zhang and Chen 2013). These observations lend further support to this model and suggest that the genetic interactions between these RBPs could be complex and context dependent.

Lastly, it is possible that some KH domain-containing RBPs may directly interact with protein components of the miRNA pathway to modulate target gene expression. Several proteins contain additional domains that are predicted to have RNA-binding activity (SAM, zinc finger, splicing factor helix hairpin) (Figure 9) and could mediate interactions among proteins and RNA. Other functional domains such as prion-like or low complexity domains were present in approximately 50% of the RBPs tested. These domains have been implicated in driving liquid phase separation and formation of protein aggregates and RNPs (Putnam *et al.* 2019). We also see several examples of domains critical for protein-protein interactions, notably the TUDOR domain present in AKAP-1, the STAR homodimerization domains present ASD-2 and GLD-1, and the ankyrin repeats in VGLN-1. Some KH domain-containing RBPs may alter the activity of miRISC by bridging essential protein components or by recruiting additional regulatory factors (Figure 10F). This model is supported by the observation that eight of the twenty-nine KH domain-containing RBPs were previously found to physically interact with miRISC components or DCR-1 (Table 3). MASK-1, FUBL-1, -2, and -3 co-precipitate with AIN-1 (Wu *et al.* 2017), whereas HRPK-1 and IMPH-1 co-precipitate with DCR-1 (Duchaine *et al.* 2006) and ALG-1 (Zinovyeva *et al.* 2015). GLD-1 was found to co-precipitate with ALG-1 (Akay *et al.* 2013; Zinovyeva *et al.* 2015) and AIN-2 (Zhang *et al.* 2007). These proteins may act as scaffolds for the formation of RNP complexes, bridging RNA components (mRNA or miRNA) miRNA biogenesis factors or miRISC (Figure 10F). Overall, KH RBPs could act directly on miRNA targets (Figure 10B) via the suggested mechanisms (Figure 10, A–D) or could indirectly coordinate with miRNAs in regulating gene expression through one or more intermediates (Figure 10A).

Table 3 Several KH domain containing RBPs physically interact with miRISC components

Gene	miRISC or biogenesis component
mask-1	AIN-1[a]
fubl-1	AIN-1[a]
fubl-2	AIN-1[a]
fubl-3	AIN-1[a]
hrpk-1	ALG-1[b], DCR-1[c]
imph-1	ALG-1[b], DCR-1[c]
gld-1	ALG-1, [b] AIN-2[d]

[a] Wu *et al.* (2017).
[b] Zinovyeva *et al.* (2015).
[c] Duchaine *et al.* (2006).
[d] Zhang *et al.* (2007).

Overall, our screen showed that many of the KH domain-containing RBPs in *C. elegans* functionally interact with miRNA-mediated regulation of gene expression. Further work is essential to characterize the mechanisms through which individual KH domain proteins may affect gene expression and how they might functionally intersect with miRNA pathways. This study highlights a number of candidates for future genetic, molecular, and biochemical characterization and shows the extent to which miRNAs and KH domain RBPs may directly or indirectly coordinate to ultimately regulate gene expression.

Acknowledgments

We thank the Zinovyeva lab for helpful technical discussions and assistance. We are grateful to Xantha Karp for critical reading of this manuscript and sharing reagents. We thank Erik Lundquist and Helge Grosshans for sharing reagents and strains. Some of the strains used in this study were provided by the CGC, which is funded by NIH Office of Research Infrastructure Programs (P40 OD010440). We thank Wormbase for providing the various necessary resources.

Funding

This paper was funded by NIH National Institute of General Medical Sciences R35GM124828 (A. Z.).

Conflicts of interest: None declared.

Literature cited

Abbott AL, Alvarez-Saavedra E, Miska EA, Lau NC, Bartel DP, *et al.* 2005. The let-7 MicroRNA family members mir-48, mir-84, and mir-241 function together to regulate developmental timing in *Caenorhabditis elegans*. Dev Cell. 9:403–414.

Abrahante JE, Daul AL, Li M, Volk ML, Tennessen JM, *et al.* 2003. The *Caenorhabditis elegans* hunchback-like gene lin-57/hbl-1 controls developmental time and is regulated by microRNAs. Dev Cell. 4: 625–637.

Akay A, Craig A, Lehrbach N, Larance M, Pourkarimi E, *et al.* 2013. RNA-binding protein GLD-1/quaking genetically interacts with the mir-35 and the let-7 miRNA pathways in *Caenorhabditis elegans*. Open Biol. 3:130151.

Alles J, Fehlmann T, Fischer U, Backes C, Galata V, *et al.* 2019. An estimate of the total number of true human miRNAs. Nucleic Acids Res. 47:gkz097.

Ambros V, Ruvkun G. 2018. Recent molecular genetic explorations of *Caenorhabditis elegans* microRNAs. Genetics. 209:651–673.

Chu JS-C, Chua S-Y, Wong K, Davison AM, Johnsen R, *et al.* 2014. High-throughput capturing and characterization of mutations in essential genes of *Caenorhabditis elegans*. BMC Genomics. 15:361.

Darbelli L, Richard S. 2016. Emerging functions of the quaking RNA-binding proteins and link to human diseases. Wires RNA. 7: 399–412.

Dassi E. 2017. Handshakes and fights: the regulatory interplay of RNA-binding proteins. Frontiers Mol Biosci. 4:67.

Dominguez D, Freese P, Alexis MS, Su A, Hochman M, *et al.* 2018. Sequence, structure, and context preferences of human RNA binding proteins. Mol Cell. 70:854–867.e9.

Duchaine TF, Wohlschlegel JA, Kennedy S, Bei Y, Conte D, *et al.* 2006. Functional proteomics reveals the biochemical niche of *C. elegans* DCR-1 in multiple small-RNA-mediated pathways. Cell. 124: 343–354.

Ecsedi M, Rausch M, Großhans H. 2015. The let-7 microRNA directs vulval development through a single target. Dev Cell. 32:335–344.

Gebert LFR, MacRae IJ. 2019. Regulation of microRNA function in animals. Nat Rev Mol Cell Biol. 20:21–37.

Gerstberger S, Hafner M, Tuschl T. 2014. A census of human RNA-binding proteins. Nat Rev Genet. 15:829–845.

Geuens T, Bouhy D, Timmerman V. 2016. The hnRNP family: insights into their role in health and disease. Hum Genet. 135: 851–867.

Goh W-SS, Seah JWE, Harrison EJ, Chen C, Hammell CM, *et al.* 2014. A genome-wide RNAi screen identifies factors required for distinct stages of *C. elegans* piRNA biogenesis. Gene Dev. 28:797–807.

Grishin NV. 2001. KH domain: one motif, two folds. Nucleic Acids Res. 29:638–643.

Grishok A, Sinskey JL, Sharp PA. 2005. Transcriptional silencing of a transgene by RNAi in the soma of *C. elegans*. Gene Dev. 19: 683–696.

Hammell CM, Lubin I, Boag PR, Blackwell TK, Ambros V. 2009. *nhl-2* modulates microRNA activity in *Caenorhabditis elegans*. Cell. 136: 926–938.

Han S, Kim D, Shivakumar M, Lee Y-J, Garg T, *et al.* 2018. The effects of alternative splicing on miRNA binding sites in bladder cancer. PLoS One. 13:e0190708.

Heintz C, Doktor TK, Lanjuin A, Escoubas CC, Zhang Y, *et al.* 2017. Splicing factor 1 modulates dietary restriction and TORC1 pathway longevity in *C. elegans*. Nature. 541:102–106.

Hernández G, Miron M, Han H, Liu N, Magescas J, *et al.* 2013. Mextli Is a novel eukaryotic translation initiation factor 4e-binding protein that promotes translation in *Drosophila melanogaster*. Mol Cell Biol. 33:2854–2864.

Hunt-Newbury R, Viveiros R, Johnsen R, Mah A, Anastas D, *et al.* 2007. High-throughput in vivo analysis of gene expression in *Caenorhabditis elegans*. PLoS Biol. 5:e237.

Janga SC. 2012. From specific to global analysis of posttranscriptional regulation in eukaryotes: posttranscriptional regulatory networks. Brief Funct Genomics. 11:505–521.

Johnston RJ, Hobert O. 2003. A microRNA controlling left/right neuronal asymmetry in *Caenorhabditis elegans*. Nature. 426:845–849.

Kaletsky R, Yao V, Williams A, Runnels AM, Tadych A, *et al.* 2018. Transcriptome analysis of adult *Caenorhabditis elegans* cells

reveals tissue-specific gene and isoform expression. PLoS Genet. 14:e1007559.

Kamath RS, Fraser AG, Dong Y, Poulin G, Durbin R, *et al.* 2003. Systematic functional analysis of the *Caenorhabditis elegans* genome using RNAi. Nature. 421:231–237.

Kamath RS, Martinez-Campos M, Zipperlen P, Fraser AG, Ahringer J. 2000. Effectiveness of specific RNA-mediated interference through ingested double-stranded RNA in *Caenorhabditis elegans*. Genome Biol. 2:research0002.1.

Kapelle WS, Reinke V. 2011. *C. elegans* meg-1 and meg-2 differentially interact with nanos family members to either promote or inhibit germ cell proliferation and survival. Genesis. 49: 380–391.

Kato M, Han TW, Xie S, Shi K, Du X, *et al.* 2012. Cell-free formation of RNA granules: low complexity sequence domains form dynamic fibers within hydrogels. Cell. 149:753–767.

Kim JK, Gabel HW, Kamath RS, Tewari M, Pasquinelli A, *et al.* 2005. Functional genomic analysis of RNA interference in *C. elegans*. Science. 308:1164–1167.

Kosugi S, Hasebe M, Tomita M, Yanagawa H. 2009. Systematic identification of cell cycle-dependent yeast nucleocytoplasmic shuttling proteins by prediction of composite motifs. Proc Natl Acad Sci U S A. 106:10171–10176.

Kumar S, Stecher G, Li M, Knyaz C, Tamura K. 2018. MEGA X: molecular evolutionary genetics analysis across computing platforms. Mol Biol Evol. 35:1547–1549.

Kuroyanagi H. 2013. Switch-like regulation of tissue-specific alternative pre-mRNA processing patterns revealed by customized fluorescence reporters. Worm. 2:e23834.

Lancaster AK, Nutter-Upham A, Lindquist S, King OD. 2014. PLAAC: a web and command-line application to identify proteins with prion-like amino acid composition. Bioinformatics. 30:2501–2502.

Letunic I, Bork P. 2017. 20 years of the SMART protein domain annotation resource. Nucleic Acids Res. 46:gkx922.

Li L, Veksler-Lublinsky I, Zinovyeva A. 2019. HRPK-1, a conserved KH-domain protein, modulates microRNA activity during *Caenorhabditis elegans* development. PLoS Genet. 15:e1008067.

Lin S-Y, Johnson SM, Abraham M, Vella MC, Pasquinelli A, *et al.* 2003. The *C. elegans* hunchback homolog, *hbl-1*, controls temporal patterning and is a probable MicroRNA target. Dev Cell. 4:639–650.

Ma L, Horvitz HR. 2009. Mutations in the *Caenorhabditis elegans* U2AF large subunit UAF-1 alter the choice of a 3′ splice site in vivo. PLoS Genet. 5:e1000708.

Marin VA, Evans TC. 2003. Translational repression of a *C. elegans* Notch mRNA by the STAR/KH domain protein GLD-1. Development. 130:2623–2632.

Nabel-Rosen H, Volohonsky G, Reuveny A, Zaidel-Bar R, Volk T. 2002. Two isoforms of the *Drosophila* RNA binding protein, how, act in opposing directions to regulate tendon cell differentiation. Dev Cell. 2:183–193.

Nicastro G, Taylor IA, Ramos A. 2015. KH–RNA interactions: back in the groove. Curr Opin Struct Biol. 30:63–70.

Nika L, Gibson T, Konkus R, Karp X. 2016. Fluorescent beads are a versatile tool for staging *Caenorhabditis elegans* in different life histories. G3 (Bethesda). 6:1923–1933.

O'Brien J, Hayder H, Zayed Y, Peng C. 2018. Overview of microRNA biogenesis: mechanisms of actions, and circulation. Front Endocrinol. 9:402.

Ohno G, Hagiwara M, Kuroyanagi H. 2008. STAR family RNA-binding protein ASD-2 regulates developmental switching of mutually exclusive alternative splicing *in vivo*. Gene Dev. 22:360–374.

Palmer RE, Inoue T, Sherwood DR, Jiang LI, Sternberg PW. 2002. *Caenorhabditis elegans cog-1* locus encodes GTX/Nkx6.1 homeodomain proteins and regulates multiple aspects of reproductive system development. Dev Biol. 252:202–213.

Parry DH, Xu J, Ruvkun G. 2007. A whole-genome RNAi screen for *C. elegans* miRNA pathway genes. Curr Biol. 17:2013–2022.

Putnam A, Cassani M, Smith J, Seydoux G. 2019. A gel phase promotes condensation of liquid P granules in *Caenorhabditis elegans* embryos. Nat Struct Mol Biol. 26:220–226.

Reinhart BJ, Slack FJ, Basson M, Pasquinelli AE, Bettinger JC, *et al.* 2000. The 21-nucleotide *let-7* RNA regulates developmental timing in *Caenorhabditis elegans*. Nature. 403:901–906.

Reinke AW, Mak R, Troemel ER, Bennett EJ. 2017. In vivo mapping of tissue- and subcellular-specific proteomes in *Caenorhabditis elegans*. Sci Adv. 3:e1602426.

Rino J, Desterro JMP, Pacheco TR, Gadella TWJ, Carmo-Fonseca M. 2008. Splicing factors SF1 and U2AF associate in extraspliceosomal complexes. Mol Cell Biol. 28:3045–3057.

Rual J-F, Ceron J, Koreth J, Hao T, Nicot A-S, *et al.* 2004. Toward improving *Caenorhabditis elegans* phenome mapping with an ORFeome-based RNAi library. Genome Res. 14:2162–2168.

Schwamborn JC, Berezikov E, Knoblich JA. 2009. The TRIM-NHL protein TRIM32 activates microRNAs and prevents self-renewal in mouse neural progenitors. Cell. 136:913–925.

Shin Y, Brangwynne CP. 2017. Liquid phase condensation in cell physiology and disease. Science. 357:eaaf4382.

Siomi H, Matunis MJ, Michael WM, Dreyfuss G. 1993. The pre-mRNA binding K protein contains a novel evolutionary conserved motif. Nucl Acids Res. 21:1193–1198.

Slack FJ, Basson M, Liu Z, Ambros V, Horvitz HR, *et al.* 2000. The *lin-41* RBCC gene acts in the *C. elegans* heterochronic pathway between the let-7 regulatory RNA and the LIN-29 transcription factor. Mol Cell. 5:659–669.

Sönnichsen B, Koski LB, Walsh A, Marschall P, Neumann B, *et al.* 2005. Full-genome RNAi profiling of early embryogenesis in *Caenorhabditis elegans*. Nature. 434:462–469.

Tabach Y, Billi AC, Hayes GD, Newman MA, Zuk O, *et al.* 2013. Identification of small RNA pathway genes using patterns of phylogenetic conservation and divergence. Nature. 493:694–698.

Tamburino AM, Ryder SP, Walhout AJM. 2013. A compendium of *Caenorhabditis elegans* RNA binding proteins predicts extensive regulation at multiple levels. G3 (Bethesda). 3:297–304.

Tsukamoto T, Gearhart MD, Spike CA, Huelgas-Morales G, Mews M, *et al.* 2017. LIN-41 and OMA ribonucleoprotein complexes mediate a translational repression-to-activation switch controlling oocyte meiotic maturation and the oocyte-to-embryo transition in *Caenorhabditis elegans*. Genetics. 206:2007–2039.

Tüfekci KU, Öner MG, Meuwissen RLJ, Genç Ş. 2013. miRNomics: microRNA biology and computational analysis. Methods Mol Biol. 1107:33–50.

Valverde R, Edwards L, Regan L. 2008. Structure and function of KH domains. FEBS J. 275:2712–2726.

Vasquez-Rifo A, Jannot G, Armisen J, Labouesse M, Bukhari SIA, *et al.* 2012. Developmental characterization of the microRNA-specific *C. elegans* Argonautes alg-1 and alg-2. PLoS One. 7:e33750.

Vella MC, Choi E-Y, Lin S-Y, Reinert K, Slack FJ. 2004. The *C. elegans* microRNA let-7 binds to imperfect let-7 complementary sites from the lin-41 3′UTR. Gene Dev. 18:132–137.

Wang X, Voronina E. 2020. Diverse roles of PUF proteins in germline stem and progenitor cell development in *C. elegans*. Front Cell Dev Biol. 8:29.

Wu E, Vashisht AA, Chapat C, Flamand MN, Cohen E, *et al.* 2017. A continuum of mRNP complexes in embryonic microRNA-mediated silencing. Nucleic Acids Res. 45:2081–2098.

Zabinsky RA, Weum BM, Cui M, Han M. 2017. RNA binding protein vigilin collaborates with miRNAs to regulate gene expression for *Caenorhabditis elegans* larval development. G3 (Bethesda). 7:2511–2518.

Zhang J, Chen QM. 2013. Far upstream element binding protein 1: a commander of transcription, translation and beyond. Oncogene. 32:2907–2916.

Zhang L, Ding L, Cheung TH, Dong M-Q, Chen J, *et al.* 2007. Systematic identification of *C. elegans* miRISC proteins, miRNAs, and mRNA targets by their interactions with GW182 proteins AIN-1 and AIN-2. Mol Cell. 28:598–613.

Zinovyeva AY, Bouasker S, Simard MJ, Hammell CM, Ambros V. 2014. Mutations in conserved residues of the *C. elegans* microRNA argonaute ALG-1 identify separable functions in ALG-1 miRISC loading and target repression. PLoS Genet. 10: e1004286.

Zinovyeva AY, Veksler-Lublinsky I, Vashisht AA, Wohlschlegel JA, Ambros VR. 2015. *Caenorhabditis elegans* ALG-1 antimorphic mutations uncover functions for aArgonaute in microRNA guide strand selection and passenger strand disposal. Proc Natl Acad Sci U S A. 112:E5271–E5280.

Communicating editor: J. Kim